PL-TR-
96-1175

LIGHT WEIGHT, LOW COST, HIGH EFFICIENCY SOLAR CELLS FOR SPACE PLANAR ARRAYS

Dr. David Lillington
Dr. Terry Cavicchi

Spectrolab, Inc.
12500 Gladstone Ave.
Sylmar, CA 91342

January 1997

Final Report

PHILLIPS LABORATORY
Space Technology Directorate
AIR FORCE MATERIEL COMMAND
KIRTLAND AIR FORCE BASE, NM 87117-5776

AD NUMBER

AD-B220 921

NEW LIMITATION CHANGE

TO

DISTRIBUTION STATEMENT A -
Approved for public release; Distribution unlimited.

Limitation Code: 1

FROM

DISTRIBUTION STATEMENT -

Limitation Code:

AUTHORITY

Janet E. Mosher, Phillips Lab/CA, Kirtland AFB, N.M.

PL-TR-96-1175

Using Government drawings, specifications, or other data included in this document for any purpose other than Government procurement does not in any way obligate the U.S. Government. The fact that the Government formulated or supplied the drawings, specifications, or other data, does not license the holder or any other person or corporation; or convey any rights or permission to manufacture, use, or sell any patented invention that may relate to them.

This report contains proprietary information and shall not be either released outside the government, or used, duplicated or disclosed in whole or in part for manufacture or procurement, without the written permission of the contractor. This legend shall be marked on any reproduction hereof in whole or in part.

If you change your address, wish to be removed from this mailing list, or your organization no longer employs the addressee, please notify PL/VTV, 3550 Aberdeen Ave SE, Kirtland AFB, NM 87117-5776.

Do not return copies of this report unless contractual obligations or notice on a specific document requires its return.

This report has been approved for publication.

David N. Keener

David Keener, 1Lt, USAF
Project Manager

FOR THE COMMANDER

L. Kevin Slimak

L. KEVIN SLIMAK, GM-15
Chief, Space Vehicle Technologies
Division

CHRISTINE M. ANDERSON
Director, Space Technology
Directorate

The following notice applies to any unclassified (including originally classified and now declassified) technical reports released to "qualified U.S. contractors" under the provisions of DoD Directive 5230.25, Withholding of Unclassified Technical Data From Public Disclosure.

NOTICE TO ACCOMPANY THE DISSEMINATION OF EXPORT-CONTROLLED TECHNICAL DATA

1. Export of information contained herein, which includes, in some circumstances, release to foreign nationals within the United States, without first obtaining approval or license from the Department of State for items controlled by the International Traffic in Arms Regulations (ITAR), or the Department of Commerce for items controlled by the Export Administration Regulations (EAR), may constitute a violation of law.

2. Under 22 U.S.C. 2778 the penalty for unlawful export of items or information controlled under the ITAR is up to two years imprisonment, or a fine of $100,000, or both. Under 50 U.S.C., Appendix 2410, the penalty for unlawful export of items or information controlled under the EAR is a fine of up to $1,000,000, or five times the value of the exports, whichever is greater; or for an individual, imprisonment of up to 10 years, or a fine of up to $250,000, or both.

3. In accordance with your certification that establishes you as a "qualified U.S. Contractor", unauthorized dissemination of this information is prohibited and may result in disqualification as a qualified U.S. contractor, and may be considered in determining your eligibility for future contracts with the Department of Defense.

4. The U.S. Government assumes no liability for direct patent infringement, or contributory patent infringement or misuse of technical data.

5. The U.S. Government does not warrant the adequacy, accuracy, currency, or completeness of the technical data.

6. The U.S. Government assumes no liability for loss, damage, or injury resulting from manufacture or use for any purpose of any product, article, system, or material involving reliance upon any or all technical data furnished in response to the request for technical data.

7. If the technical data furnished by the Government will be used for commercial manufacturing or other profit potential, a license for such use may be necessary. Any payments made in support of the request for data do not include or involve any license rights.

8. A copy of this notice shall be provided with any partial or complete reproduction of these data that are provided to qualified U.S. contractors.

D E S T R U C T I O N N O T I C E

For classified documents, follow the procedures in DoD 5200.22-M, Industrial Security Manual, Section II-19 or DoD 5200.1-R, Information Security Program Regulation, Chapter IX. For unclassified, limited documents, destroy by any method that will prevent disclosure of contents or reconstruction of the document.

DRAFT SF 298

1. Report Date (dd-mm-yy) January 1997	2. Report Type Final	3. Dates covered (from... to) 09/91 to 09/96
4. Title & subtitle Light Weight, Low Cost, High Efficiency Solar Cells for Space Planar Arrays		5a. Contract or Grant # F33615-91-C-2146
		5b. Program Element # 63401F
6. Author(s) Dr. David Lillington Dr. Terry Cavicchi		5c. Project # 682J
		5d. Task # TD
		5e. Work Unit # SL
7. Performing Organization Name & Address Spectrolab, Inc. 12500 Gladstone Ave. Sylmar, CA 91342		8. Performing Organization Report #
9. Sponsoring/Monitoring Agency Name & Address Phillips Laboratory 3550 Aberdeen Ave. SE Kirtland AFB, NM 87117-5776		10. Monitor Acronym
		11. Monitor Report # PL-TR-96-1175

12. Distribution/Availability Statement
Distribution authorized to U.S. Government agencies only; Proprietary Information; January 1997. Other requests for this document shall be referred to Phillips Laboratory/VTV, 3550 Aberdeen Ave. SE, Kirtland AFB, NM 87117-5776.

13. Supplementary Notes

14. Abstract The objective of the High Efficiency Solar Cell Program was to develop a cost effective, high efficiency solar cell that could be easily integrated into existing Air Force space systems to provide increased BOL and EOL efficiency. Gallium arsenide (GaAs) solar cells at 18% efficiency are state-of-the-art; this program desired to increase the solar conversion efficiency of solar cells to >20%. Spectrolab, Inc. met this objective with a GaInP/GaAs/Ge triple junction solar cell structure, which successfully demonstrated AM0, 28°C efficiencies up to 23.3% for a 2x2 cm solar cell. The lot average efficiency of 75 cells delivered to the Air Force was 22.0%. The triple junction cell was developed in two parts, a GaInP/GaAs tandem cell and Ge bottom cell. At the end of the program, the top tandem cell was capable of contributing 22% to the overall cell efficiency and the Ge cell was capable of contributing 1.9%. The cells were extensively tested, including electron radiation, temperature coefficient, 30 day humidity tests, and thermal vacuum cycling to show that these cells were a viable direct replacement for GaAs cells and capable of operating in nominal space environments.

15. Subject Terms Multijunction solar cells, Photovoltaics, Space Power, Energy Generation, Electrical Power

Security Classification of			19. Limitation of Abstract	20. # of Pages	21. Responsible Person (Name and Telephone #)
16. Report Unclassified	17. Abstract Unclassified	18. This Page Unclassified	limited	56	1Lt David Keener (505) 846-5393

CONTENTS

CONTENTS (Concluded)

FIGURES

FIGURES (Continued)

FIGURES (Concluded)

TABLES

1.0 EXECUTIVE SUMMARY

This final technical report summarizes the work performed on AF contract No. F33615-91-C-2146. In this program, $GaInP_2$/GaAs/Ge monolithic triple junction solar cells were successfully demonstrated and an AM0, 28 °C efficiency of 23.3% was achieved for a cell measuring 2 cm x 2 cm. At the time of fabrication, this efficiency was the highest reported for a monolithic, triple junction cell. Over the period of the contract, a total of seventy-five (75), 2 cm x 2 cm bare cells and fifty-two (52) 2 cm x 2 cm cell-interconnect-cover (CIC) assemblies were delivered to Phillips Laboratory. The average AM0, 28 °C efficiency for the seventy-five cells and fifty-two CICs were 22.0% and 21.9%, respectively.

Throughout the period of development, electron irradiation, temperature coefficient, and 30 day humidity tests were periodically performed to characterize bare cells. CICs were also subjected to thermal cycling to verify the space flight worthiness of the composite welded CIC assembly. A triple junction cell was also flown and tested on the 1995 Jet Propulsion Laboratory (JPL) balloon flight, as a verification of ground measurement accuracy. The flight test data confirmed, to within reasonable accuracy, the ground measurements made by both National Renewable Energy Laboratory (NREL) and Spectrolab.

"On-orbit" modeling, based on theoretical and experimentally measured temperature coefficients, was performed to calculate triple junction cell performance at elevated temperatures. The preliminary analysis confirmed that, although the rate of change of efficiency with temperature is relatively high compared to single junction GaAs/Ge cells (due to the low band gap of Ge), there is a net benefit to on orbit operating efficiency in geosynchronous orbits where operating temperatures are in the range 50 °C to 60 °C. The triple junction solar cell, when developed to a state of full flight readiness, should therefore find widespread application in many government flight systems requiring higher power density than is currently available today.

2.0 INTRODUCTION

2.1 TECHNICAL OBJECTIVES

The overall objective for this program was to develop a cost effective, high efficiency solar cell that can be easily integrated into existing Air Force space power systems to provide increased BOL and EOL performance. The technical objectives of the program were as follows:

1. Demonstrate a proof-of-concept, two-terminal, weldable, triple junction solar cell that was scaleable in size and could be manufactured using low cost materials and processes, at high yield
2. Deliver cells for Air Force evaluation with a BOL goal efficiency of 24%, measured at AM0, 28 °C
3. Achieve 80% of BOL power at an End Of Life (EOL) mission requirement of $1x10^{15}$, 1MeV electrons/cm,
4. Demonstrate a device that was thermally stable in "threat environments" in which temperatures up to 425 °C would be experienced for limited periods
5. Develop a cell design that enabled high panel specific power (>80W/Kg) when used with existing substrates and cell covers (filters) designed for geosynchronous orbit

2.2 TECHNICAL APPROACH

Spectrolab's approach to achieving the overall objectives of this program was to develop a monolithic, two terminal, triple junction $GaInP_2$/GaAs/Ge solar cell. This design was believed to be the lowest risk approach to cost effective manufacturing of large area solar cells, with the potential to achieve minimum average efficiencies in excess of 24%.

A cross sectional view of the triple junction cell is shown in Figure 1. Although very early program efforts focused on an approach of mechanically stacking a dual junction $GaInP_2$/GaAs

cell on top of a discrete Ge cell, the program was quickly redirected to the fully monolithic design shown in the figure when it became apparent that a second tunnel junction could be used to connect three cells together in a two-terminal monolithic configuration.

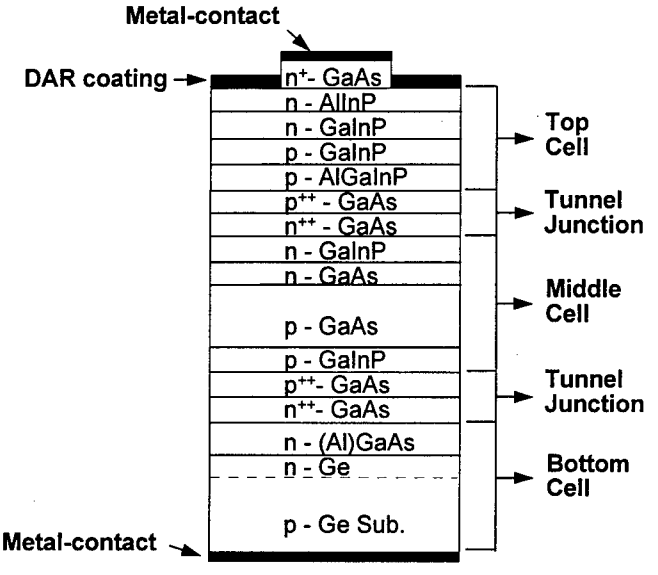

Figure 1 Cross-section of a $GaInP_2$/GaAs/Ge triple junction solar cell. Active regions designed for current matched operation for maximum efficiency. Front cap contact provides assembly hardness for panel integration.

The principal features of triple junction cell design, beginning at the p-type Ge substrate were as follows:

1. An n-type GaAs layer grown on the p-type Ge wafer, of sufficient thickness to ensure nearly defect free subsequent layers. In addition to buffering defects, the GaAs served as a source of As that diffused much more rapidly than Ga into the Ge wafer to form the active n/p junction. Furthermore, the GaAs layer was used to passivate the Ge emitter surface so that relatively low Ge saturation currents (and high Ge cell V_{oc} and efficiency) could be achieved
2. A heavily doped p^{++}/n^{++} GaAs tunnel junction (PRTJ) to provide low electrical resistance between the active Ge cell and the GaAs cell
3. A GaAs bottom cell responding to light in nominally the 0.67-0.90 μm wavelength range

4. A heavily doped p^{++}/n^{++} GaAs Inter Connect Tunnel Junction (ICTJ) to electrically connect the GaAs cell to the $GaInP_2$ top cell
5. A $GaInP_2$ top cell responding to light in nominally the 0.35-0.67 μm wavelength range, and
6. A GaAs layer capping the $AlInP_2$ window layer of the top cell.

Electrical contacts to the cell were comprised of Ti/Au/Ag for the front n-contact, and Au/Ni/Ag for the rear contact to the Ge substrate. Each contact system was selected for its environmental stability and suitability for welded cell integration. A dual layer antireflection (DAR) coating of TiO_2 and Al_2O_3 was also applied to the cell in thicknesses optimized for the glass filtered condition.

During the early stages of the program a small scale research MOVPE reactor was utilized for the growth of $GaInP_2$ material for dual junction $GaInP_2$/GaAs cell development. This technology was later transferred to a medium scale multi-wafer, horizontal reactor, and ultimately, in the later stages of the program, into a high volume, multi-wafer, Turbo Disc Reactor™ (TDR) termed the Enterprise 400. The MOVPE FAB 1 manufacturing area is shown in Figure 2 and a more detailed perspective of the reactor is shown in Figure 3.

The Turbo Disc Reactor™ systems offer significant advantages for manufacturing multjunction solar cells in high volume since they incorporate fully automated, cassette to cassette loading and unloading of wafers from within the reactor. A total of ninety (90) 100 mm diameter wafers can be processed without breaking vacuum. Additionally, the systems achieve approximately a ten-fold improvement in compositional, and thickness uniformity compared to previous barrel reactor designs, through the implementation of improved gas dynamics in the equipment design. This aspect is particularly crucial for controlling tunnel junction doping concentration and thickness, and also in reproducibly controlling the composition and thickness of the $GaInP_2$ top cell in the monolithic triple junction solar cell stack.

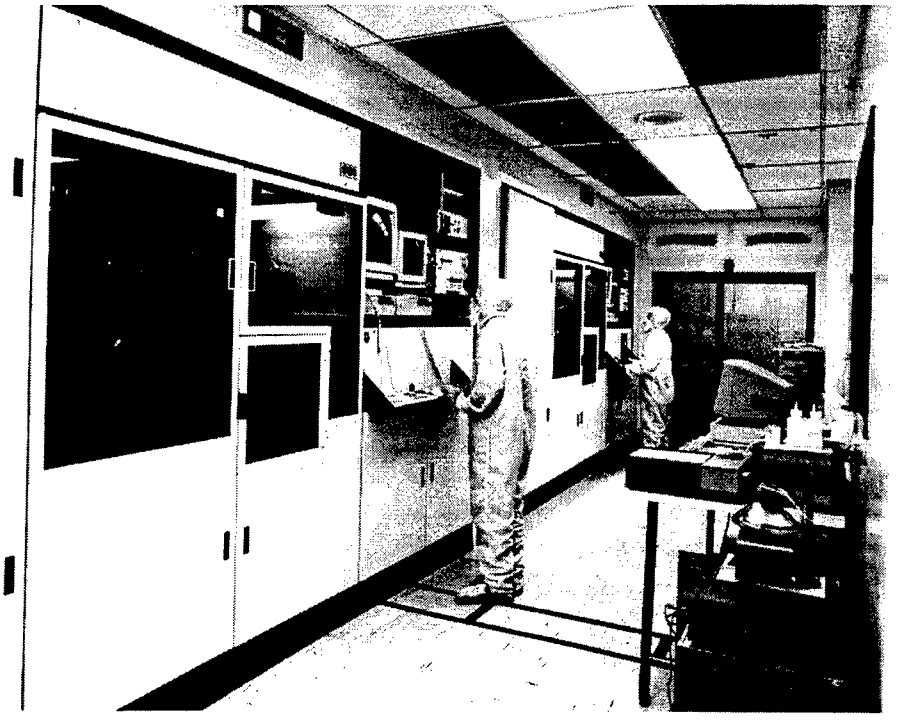

Figure 2. Enterprise 400 MOVPE manufacturing systems located in Spectrolab FAB 1 area.

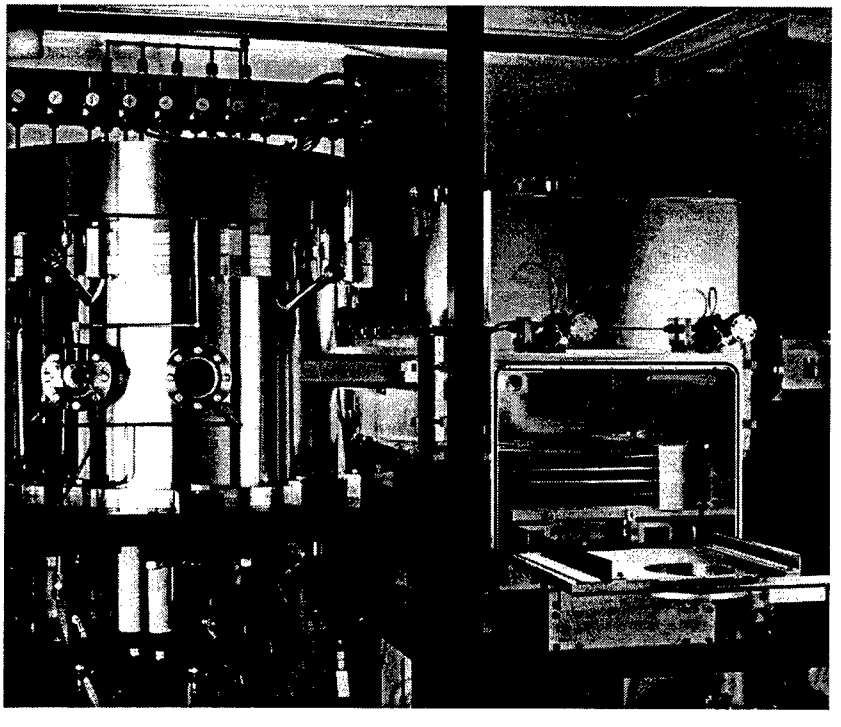

Figure 3. Close up view of Enterprise 400 system showing reactor vessel and load lock

3.0 TECHNICAL DISCUSSION

3.1 $GaInP_2$/GaAs DUAL JUNCTION CELL DEVELOPMENT

As previously mentioned, the early stages of the program focused on the development of device structures and processes for fabricating dual junction $GaInP_2$/GaAs cells. A cross section of the dual junction cell is shown in Figure 4. The thickness of the emitter and base layers in the top cell were typically 0.1-0.15 μm and 0.4-0.48 μm, respectively. The carrier concentration in the emitter of both cells was 1-3x10^{18} cm^{-3}. The base of the top cell was doped to a level of 1-3 x10^{17} cm^{-3}, while a base doping of the 3-6 x 10^{16} cm^{-3} was used in the GaAs cell to maximize EOL current collection and hence meet the EOL performance goal. A high bandgap $AlInP_2$ layer was used to passivate the front of the $GaInP_2$ cell; the back surface was passivated in these cells with an AlGaInP layer.

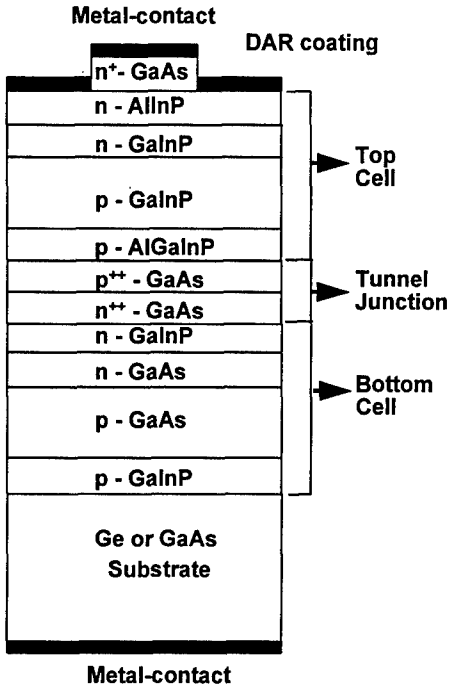

Figure 4. Cross-section of $GaInP_2$/GaAs/Ge dual junction cell.

A $GaInP_2$ layer was used both for the window and a back surface field layers (BSF) on the GaAs cell. The principal difference in features between the dual and triple junction designs was that an n-type Ge wafer was used for the dual junction cell and a p-type wafer was used for the triple junction cell. The MOVPE process for initial GaAs nucleation in the triple junction cell was also chosen so that there was arsenic diffusion into the substrate, thereby forming an n/p junction in the Ge substrate. Other layers, previously described for the triple junction cell in items 2 through 6 of Section 2.2, were identical both in terms of physical characteristics and electrical function.

In order to facilitate the cell development process, and minimize the number of variable parameters, dual junction $GaInP_2$/GaAs cell growths were initially performed on GaAs substrates. During this phase, an AM0, 28 °C efficiency of 21.9% was demonstrated on a cell without back surface field. Calculations indicated that the incorporation of a BSF in the top cell would have increased this to 22.6%. Dual junction cell optimization was then continued using Ge substrates. During this phase an AM0, 28 °C efficiency of 24.2% was achieved for a relatively small area 0.5 cm x 0.5 cm cell. This was the first demonstration, and highest reported efficiency at that time, for an n/p $GaInP_2$/GaAs dual junction cell, grown on an inactive Ge substrate.

Section 3.1.1 below describes the work that was performed to grow dual junction cells, first on GaAs substrates, and then subsequently on Ge substrates.

3.1.1 Dual-Junction $GaInP_2$/GaAs Cell Growths on GaAs Substrates

The structure used for this large area demonstration differed in some significant respects from that shown in Figure 4. Specifically, there was no BSF in the $GaInP_2$ top cell, the GaAs cell window was comprised of AlGaAs, the base layer of the GaAs cell was doped to a level of 1-3 x 10^{17} cm^{-3}, and there was no BSF in the GaAs cell. The GaAs substrates used were <100>, Zn-doped, and were mis-oriented, 2 degrees towards the <110> direction. The substrate diameter was 3". Although the cell design was not optimized at this point in the program, the results provided important data to assess the uniformity of layer growth over large areas in a multiple wafer reactor.

3.1.1.1 Dual Junction $GaInP_2$/GaAs/(GaAs) Cell Performance

The 3" diameter GaAs wafers were processed into 2 cm x 2 cm $GaInP_2$/GaAs/(GaAs) cells using standard GaAs cell processing techniques. The highest AM0, 28 °C efficiency measured among these cells was 21.9%. The IV curve of this cell is shown in Figure 5. The open circuit voltage (Voc), short circuit current (Isc), and curve fill factor (Cff), were 2.23 V , 63.0 mA and 84.2%, respectively. Subsequent analysis indicated that the incorporation of a BSF into the thin $GaInP_2$ cell would have increased the efficiency by a relative 2.8%, to 22.5%. The high uniformity of layer thickness across one of the best 3" diameter wafers is evident in the electrical performance data of the cells shown in Figure 6. The average cell efficiency was 21.3% and could have been as high as 21.9% if a BSF had been used, based on the previous assumption of a 2.8% increase in efficiency.

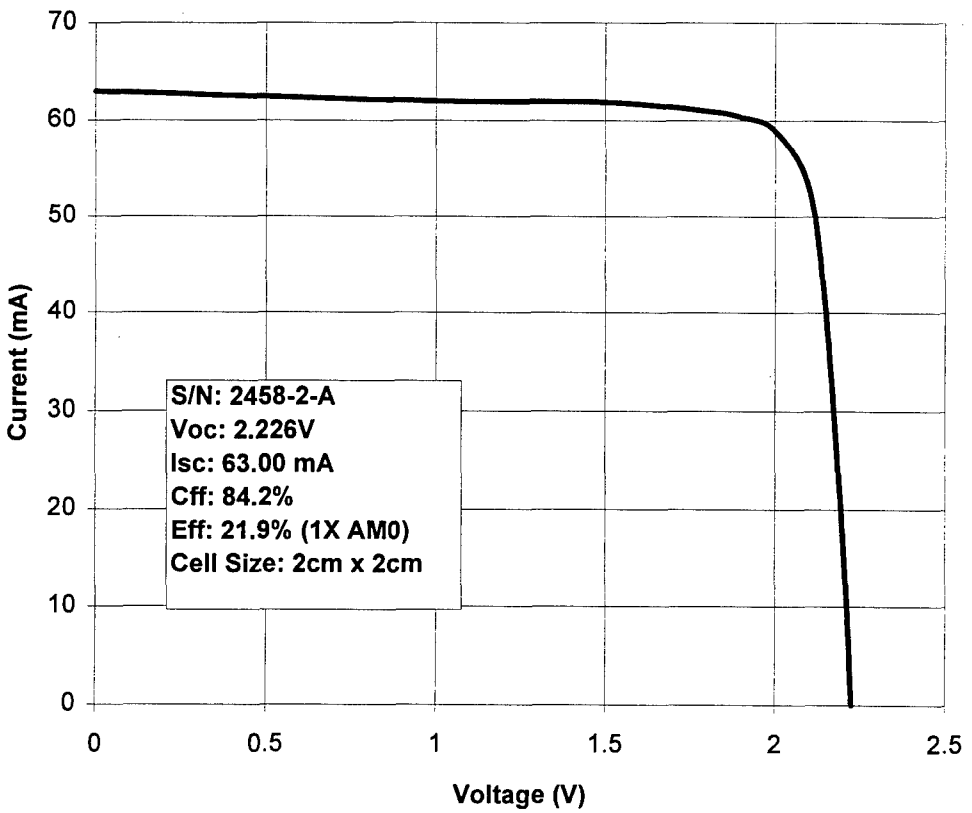

Figure 5. I-V curve for highest efficiency $GaInP_2$/GaAs/(GaAs) dual-junction cell

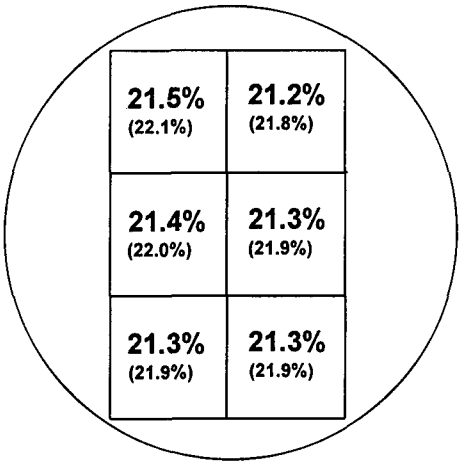

Figure 6. Measured efficiency variation of $GaInP_2$/GaAs/(GaAs) dual-junction cells across a 3" diameter GaAs substrate. Extrapolated efficiency with BSF is shown in parantheses.

3.1.1.2 Dual Junction $GaInP_2$/GaAs/(GaAs) Cell Coupon Performance

An ongoing task was to verify that the multi-junction cells, developed on this program, could be assembled into test coupons using standard panel processing techniques, without degrading device performance. Two proof-of-concept coupons, shown in Figure 7, were assembled, each using four CICs with efficiencies ranging from 18.2% to 20.9%. The cells were interconnected in series using silver plated Kovar straps, welded to the top and bottom metal contacts of the cells. CMX cover glasses 6 mil thickness were attached to cell front side using Dow Corning DC 93-500 adhesive. The coupons were then tested under a spectrally corrected X-25 simulator.

The electrical performance of the four CICs and two test coupons is summarized in Table 1. The measured Voc for the two coupons, 4.39 V and 4.43 V, was approximately equal to the sum of Voc from each component CIC in the coupon indicating that no degradation, resulting from the welding process, had occurred. The small difference in Isc and efficiency between the CICs and coupons was considered to be within the limits of measurement accuracy and repeatability.

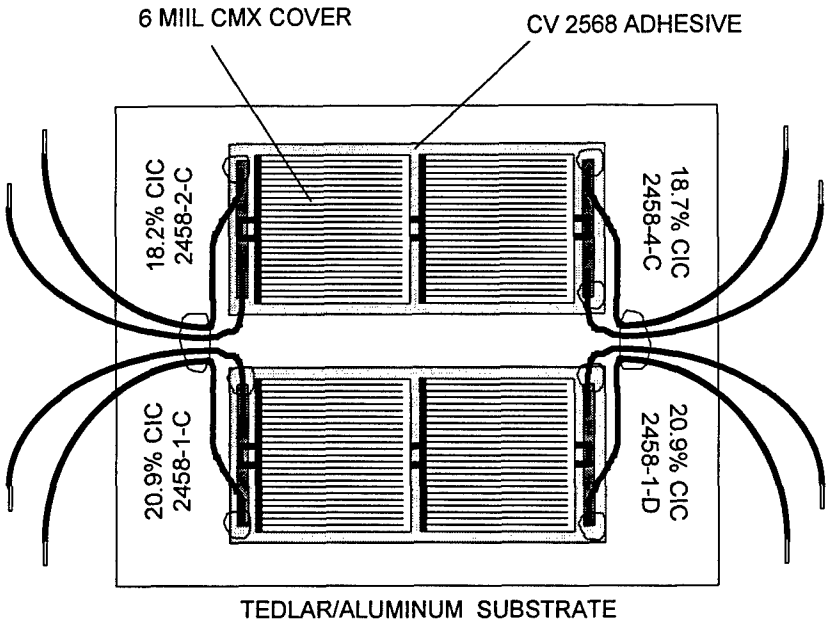

Figure 7. Proof-of-concept coupon layout. Each coupon consists of two 2 cm x 2 cm $GaInP_2$/GaAs/GaAs dual junction cells.

Table 1. Light I-V results of CICs and coupons

Cell No.	Voc (mV)	Isc (mA)	Eff (%)
2458-1-C	2225	60.21	20.9
2458-1-D	2223	60.62	20.9
Coupon 1	4434	60.16	20.8
2458-2-C	2199	60.14	18.2
2458-4-D	2205	60.15	18.7
Coupon 2	4391	60.48	18.4

3.1.2 Dual Junction $GaInP_2/GaAs/(Ge)$ Cell Growths on Ge Substrates

Having developed the MOVPE growth techniques to repeatably grow $GaInP_2/GaAs$ solar cells on GaAs substrates, the same techniques were used to grow similar device structures on 3" diameter n-type Ge substrates. A cross sectional view of the dual junction cell on an n-type Ge substrate is shown in Figure 4 and the detailed device structure has been previously described in Section 3.1. After MOVPE growth, the wafers were processed into 0.5 cm x 0.5 cm, and 1 cm x 1 cm, solar cells using standard processing techniques. After fabrication, the electrical performance of the cells was measured at both Spectrolab and National Renewal Energy Laboratory (NREL) using a spectrally modified X-25 simulator. The IV curve of the highest efficiency 0.5 cm x 0.5 cm cell was 24.2% (AM0, 28 °C) as shown in Figure 8. The Voc, Jsc, and Cff were 2.39 V, 15.93 mA/cm^2 and 86.7%, respectively.

The IV curve of the highest efficiency 1 cm x 1 cm cell, measured at NREL is shown in Figure 9. The efficiency was 22.1% and Voc, Jsc and Cff were 2.34 V, 14.99 mA/cm^2 and 85.9%, respectively. The high Voc indicated that there was no voltage drop (bucking voltage) at the GaAs/Ge interface and confirmed the absence of an active Ge junction that could have been caused by arsenic diffusion from the GaAs layers into the Ge substrate.

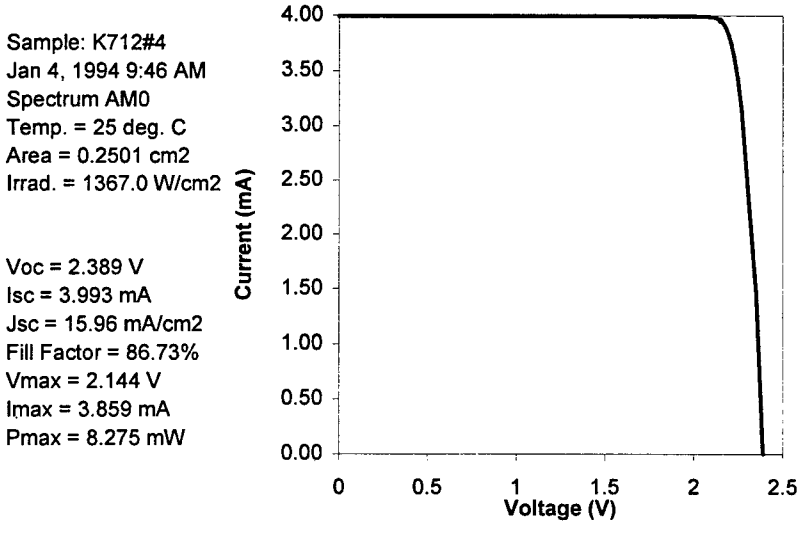

Figure 8. IV curve and data for the highest efficiency 0.5 cm x 0.5 cm $GaInP_2/GaAs/(Ge)$ dual-junction cell measured at NREL.

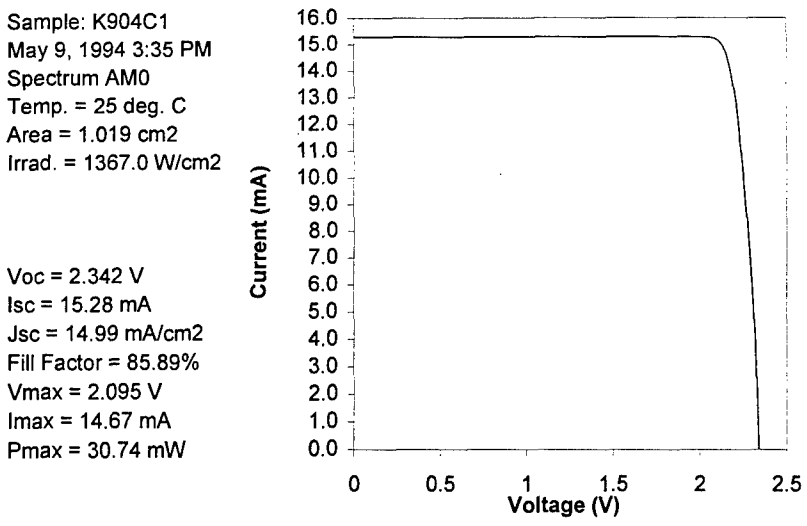

Figure 9. I-V curve of highest efficiency 1 cm x 1 cm $GaInP_2$/GaAs/(Ge) dual junction cell (S/N: K904).

3.2 Ge BOTTOM CELL DEVELOPMENT

Following the successful fabrication of dual junction $GaInP_2$/GaAs/(Ge) cells on an inactive substrate, work began to make the Ge wafer active and thereby form a triple junction cell.

The baseline design for the Ge bottom cell consisted of a p-Ge substrate, with an n-type Ge emitter and an AlGaAs (or GaAs) window layer. [The n-Ge emitter was formed by the diffusion of arsenic (As) into the p-Ge substrate during GaAs nucleation and subsequent $GaInP_2$/GaAs solar cell growth]. The most important parameters controlling Ge bottom cell performance were known to be junction depth, caused by the interdiffusion of Ga, As and Ge at the GaAs/Ge interface, emitter front surface recombination velocity, and base doping level. Extensive modeling was therefore performed using PC-1D, a one dimensional finite element analysis program, to model Ge cell performance. This was then followed by a series of MOVPE growths to optimize the stand alone single junction Ge bottom cell, prior to finally integrating all of the processing steps into the monolithic triple junction cell.

3.2.1 Ge Bottom Cell Performance Modeling Using PC-1D

The PC-1D model was setup with parameters that most closely resembled the operating conditions and fabrication parameters for Ge bottom cell. The junction depth and profile were conservatively chosen to be to approximately 3.5 μm as shown in Figure 10. The illuminating spectrum was assumed to be AM0, but filtered with GaAs (i.e. cut off at 0.9μm), amounting to an irradiance on the Ge cell of 47 mW/cm^2. The n-type window layer, serving as a front surface mirror for the minority carriers in the emitter of the Ge cell, was assumed to be AlGaAs. Figure 11 shows the band diagram for the AlGaAs layer on top of Ge junction. Two compositions of AlGaAs are shown, namely 40% and 80% Al. The difference between these compositions results a small band mismatch in conduction band while the valence band is expected to produce a strong mirror of over 1.2 eV in height.

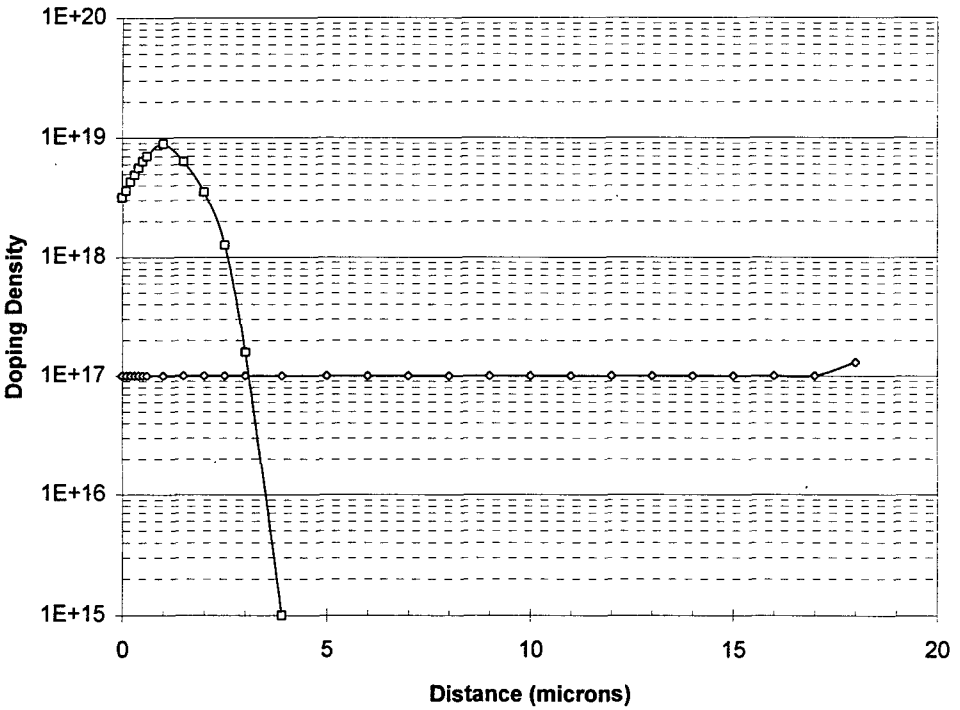

Figure 10. Modeled As diffusion profile in n/p Ge single junction cell.

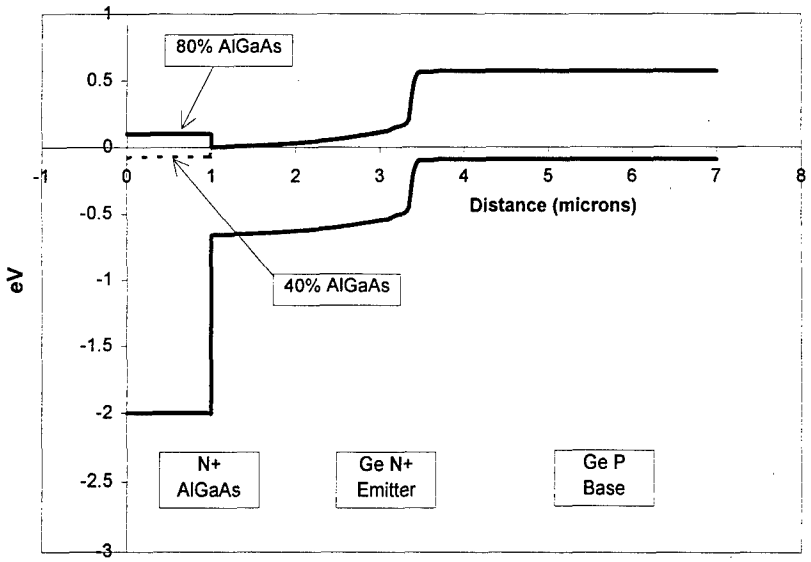

Figure 11. Energy band diagram of Ge cell passivated with AlGaAs layers of 40% and 80% composition.

Figures 12a, b and c summarize the results from the modeling in which the front surface recombination velocity on the cell was varied to assess the effect of this parameter on the variables, Voc, Isc and the maximum power (Pmax).

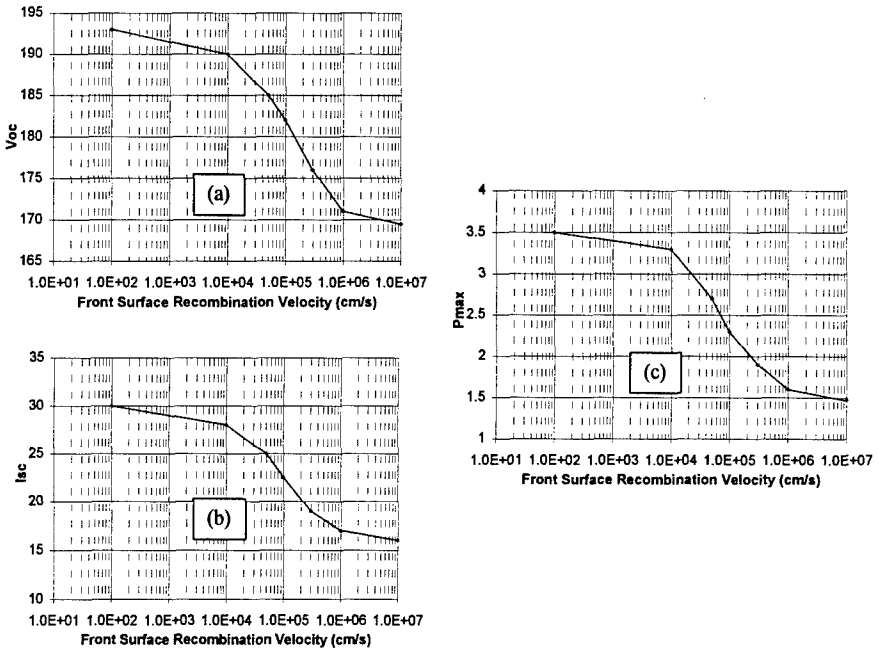

Figures 12a, b, and c. Dependence of (a) Voc, (b), Isc, and (c) Pmax, on front surface recombination velocity.

Each of these variables was found to be strongly dependent on surface recombination velocity, indicating the necessity to achieve a thin, highly passivated n-type Ge emitter at the Ge wafer surface.

3.2.2 Ge Bottom Cell Experimental Results

3.2.2.1 Ge Bottom Cell Junction Formation

Ge junction formation occurs through the diffusion of As into the p-type Ge substrate during GaAs nucleation on the Ge wafer and the subsequent $GaInP_2$/GaAs material growth. Both AsH_3 flow and growth temperature have been identified to be two major elements affecting the junction depth. In order to determine and control the As diffusion in the Ge substrate, test structures as shown in Figure 13 were first grown using a modified growth condition that formed only the Ge junction (not the complete triple junction cell structure) but simulated the thermal load that might be experienced during triple junction cell growth. Two different growth times of 10 minutes and 70 minutes were performed.

Cap	GaAs(n)	Si	3-5E18	0.5 μm
Window	$Al_{.8}Ga_{.2}As$(n)	Si	1-3E18	500 A
Base	GaAs(n)	Si	1-3E17	0.6 um
Buffer:	GaAs(n)	Si	1-3E18	0.2 um
Window :	$Al_{.4}Ga_{.6}As$(n),	Si	1-3E18	1000 A
Substrate Ge (p)				

Figure 13. Test structure for Ge bottom cell formation.

The AlGaAs and GaAs layers were then etched off and SIMS analysis was performed to determine the As profile in the Ge substrate. The SIMS data, shown in Figures 14 and 15, indicated that the As had diffused approximately 1.5 μm in 10 minutes and approximately

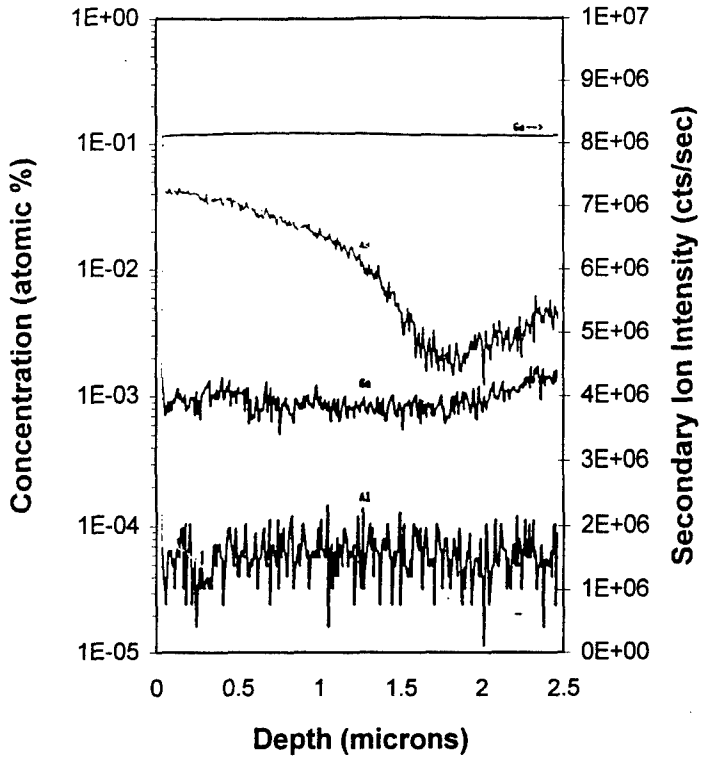

Figure 14. SIMS profile of 3M1813T3 in Ge substrate. As diffused approx. 1.5 um in 10 min.

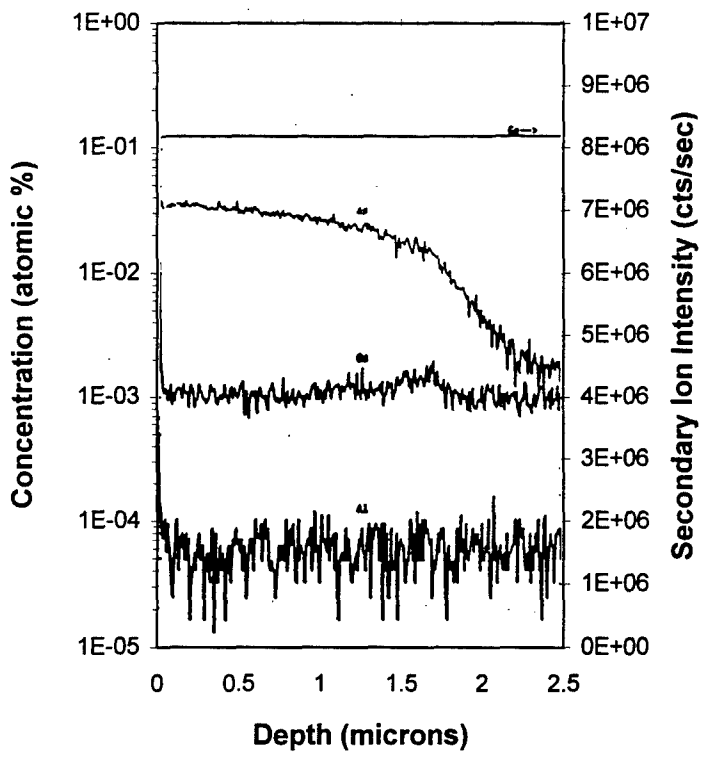

Figure 15. SIMS profile of 3M1796T3 in Ge substrate. As diffused approx. 2.5 μm in 70 min.

2.5 μm in 70 minutes. These results indicated that the Ge junction could be controlled between 1.5 μm to 2.5 υm in the Ge bottom cell under the modified growth condition. Ga or Al diffusion into the Ge substrates was undetectable in the SIMS analysis.

3.2.2.2 Ge Bottom Cell Performance

Ge bottom cells were initially fabricated using both $Al_{.40}Ga_{.60}As$, $Al_{.50}Ga_{.50}As$ and $Al_{.80}Ga_{.20}As$ for window passivations. However, the relatively high Al concentration in each device design was found to result in unacceptably high oxygen concentration in the window layer, thereby increasing surface recombination velocity and reducing cell performance. The high oxygen concentration in high Al composition layers was attributed, either to incomplete purging of the MOVPE reactor chamber prior to growth, or to bad source materials. In any case it was impossible to grow high Al composition layers with low oxygen composition so the Al concentration in the window was further lowered to $Al_{.15}Ga_{.85}As$.

In order to study the trade-off between cells with a lower oxygen concentration but lower band gap offset at the window/emitter interface (using GaAs window passivation), and a higher oxygen concentration but higher band gap offset (using $Al_{.15}Ga_{.85}As$ window passivation), additional solar cell structures, shown in Figure 16 and 17, were grown.

Cap	GaAs(n)	Si	3-5E18	0.2 μm
Base	GaAs(n)	Si	1-3E17	0.6 μm
Graded	GaAs(n)	Si	3E18 to 1E17	0.4μm
Buffer2	GaAs(n)	Si	1-3E18	0.2 μm
Window :	$Al_{.15}Ga_{.85}As$(n)	Si	1-3E18	500 A
Buffer1	GaAs(n)	Si	1-3E18	250A
Substrate Ge (p)				

Figure 16. Type-1 structure for Ge bottom cell formation.

Cap	GaAs(n)	Si	3-5E18	0.2 μm
Base	GaAs(n)	Si	1-3E17	0.6 μm
Graded	GaAs(n)	Si	3E18 to 1E17	0.4μm
Buffer2	GaAs(n)	Si	1-3E18	0.2 μm
Buffer1	GaAs(n)	Si	1-3E18	250A
Substrate Ge (p)				

Figure 17. Type-2 structure for Ge bottom cell formation.

Wafers were then processed into a 1 cm x 1 cm cells with no antireflection coating (ARC). After processing, the cells were tested under AM0 illumination using a spectrally corrected X-25 solar simulator. The simulator intensity was adjusted using a JPL balloon flight Ge standard cell (with GaAs filter). Spectral response and reflectance were also measured. The results showed that the electrical performance of the Type-2 structure (with GaAs window passivation) was much better than the Type-1 structure (with $Al_{.15}Ga_{.85}As$ window passivation), indicating that oxygen related problems at the $Al_{.15}Ga_{.85}As$/Ge interface has been the main reason for poor cell performance.

The measured IV curve of highest efficiency 1 cm x 1 cm Ge cell measured among this group of cells is shown in Figure 18. The AM0 efficiency was 1.90%. The Voc, Isc and Cff were 220.5 mV, 18.05 mA and 64.4%, respectively. Figure 19 also shows the uniform distribution of Voc and Isc across a 3 inch diameter wafer. The average Voc and Isc were 217.1 mV and 17.3 mA, respectively, in this wafer. The measured spectral response and reflectance within the spectral band 850 nm to 1850 nm, are shown in Figure 20. Without an ARC, the external quantum efficiency (Q.E.) was measured to be between 30% to 62% and the reflectance was between 25% to 46%. The internal Q.E, calculated from the external Q.E and reflectance was determined to be between 40% to 90%. This is also shown in Figure 20.

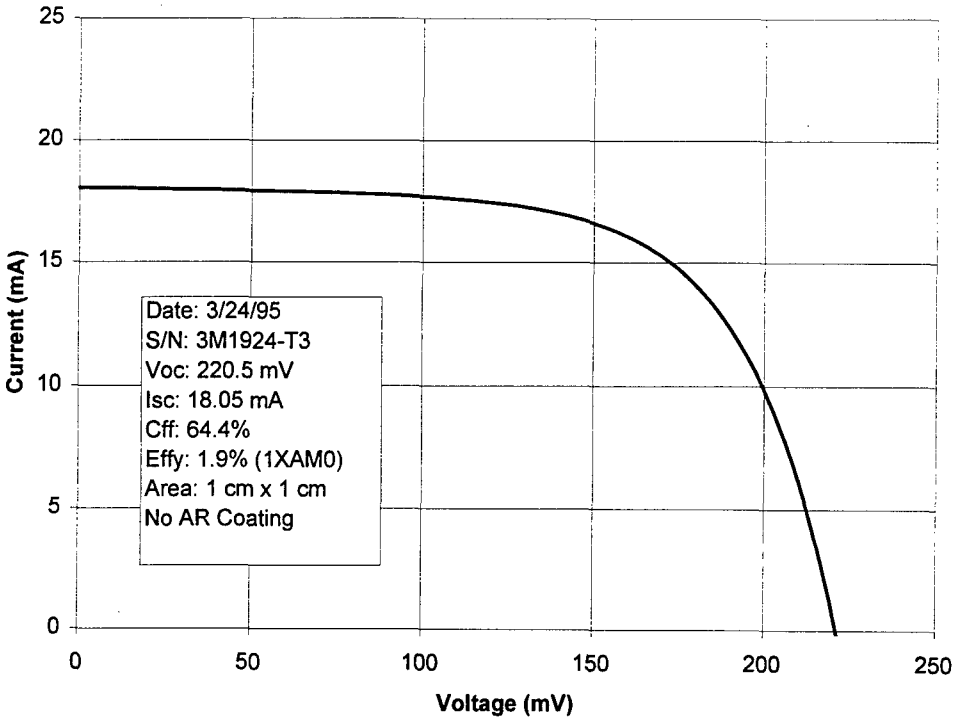

Figure 18. Light I-V curve of 1 cm x 1 cm Ge single junction cell under a 1.5 μm GaAs filter.

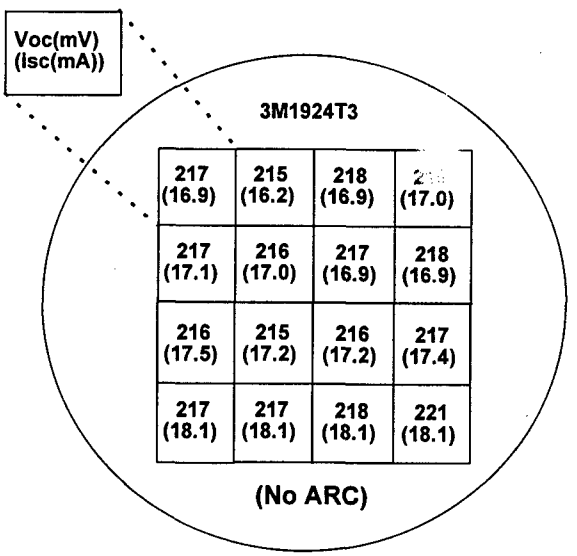

Figure 19. Voc and Isc distribution of 1 cm x 1 cm Ge single junction cells (without ARC) across a 3" diameter substrate.

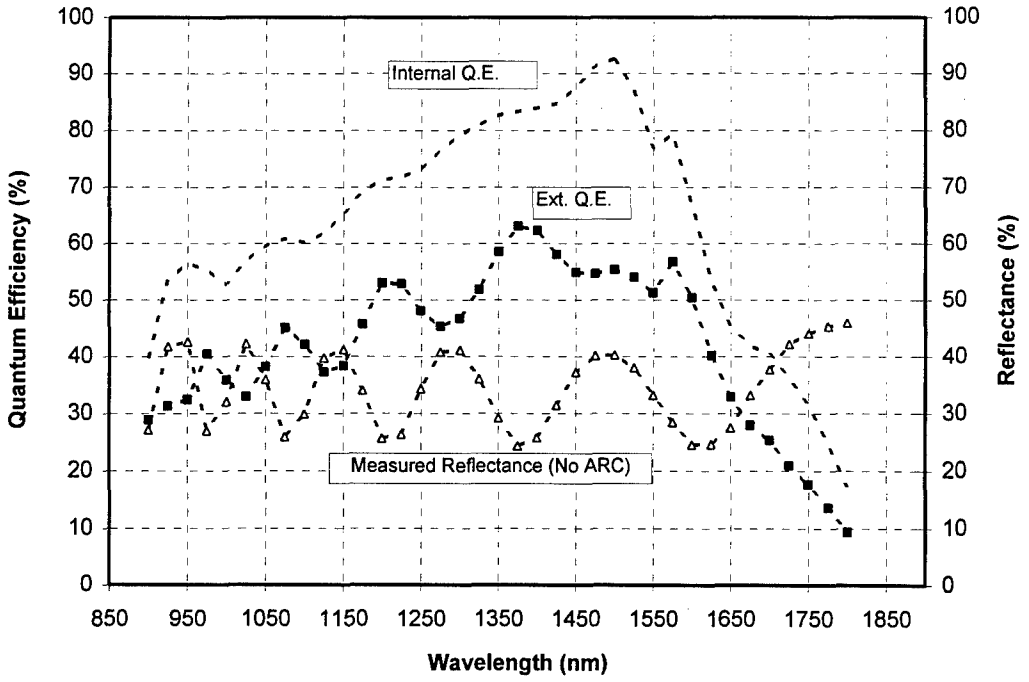

Figure 20. Measured external quantum efficiency and reflectance of a 1 cm x 1 cm Ge single junction cell without an ARC.

Since the reflectance of a triple junction cell, with ARC and coverglass, was expected to be identical to the reflectance of a dual junction cell grown on Ge substrate, the same measured reflectance curve of the dual junction cell was used to calculate the anticipated external Q.E. of the Ge cell, in a triple junction cell stack, under the same ARC and coverglass. The dual junction reflectance, internal Q.E and calculated external Q.E are shown collectively in Figure 21. The current density calculated from the integration of the external Q.E. curve of Figure 21 with the AM0 spectrum was 24.30 mA/cm^2. The calculated Ge cell current density for a triple junction cell with no AR coating was calculated to be 17.74 mA/cm^2. This result indicated that a 37% increase in current density should be experienced on a triple junction cell after application of ARC and coverglass. Using this gain factor it should ultimately possible to achieve Ge cells with about 2.60% efficiency at the maximum power point, resulting in >2% absolute efficiency gain at the operating point of the triple junction cell.

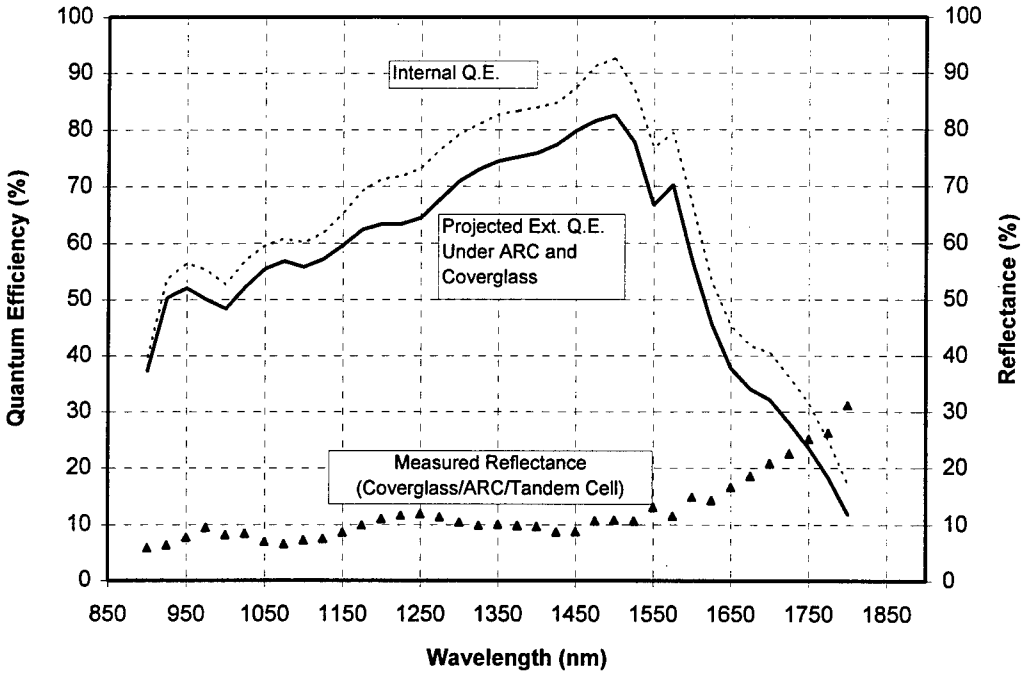

Figure 21. Projected external quantum efficiency of a 1 cm x 1 cm Ge single junction cell under an ARC and coverglass.

3.3 MONOLITHIC $GaInP_2$/GaAs/Ge TRIPLE JUNCTION CELL DEVELOPMENT

3.3.1 Triple Junction Cell Performance Modeling

Cell performance modeling was carried out to determine the minimum average efficiency expected for the triple-junction cell, manufactured in the high volume production environment. The approach used was to combine the already demonstrated empirical performance of the dual junction cell with the conservatively modeled performance for the Ge bottom cell. This was deemed to be a valid approach since the triple-junction cell structure, shown in Figure 4, essentially consists of a dual junction $GaInP_2$/GaAs cell connected in series to the Ge bottom cell through a second GaAs tunnel junction. The resulting IV curve for a triple junction $GaInP_2$/GaAs/Ge cell is shown in Figure 22. The expected minimum average efficiency at Beginning Of Life (BOL) was calculated to be 26.5%.

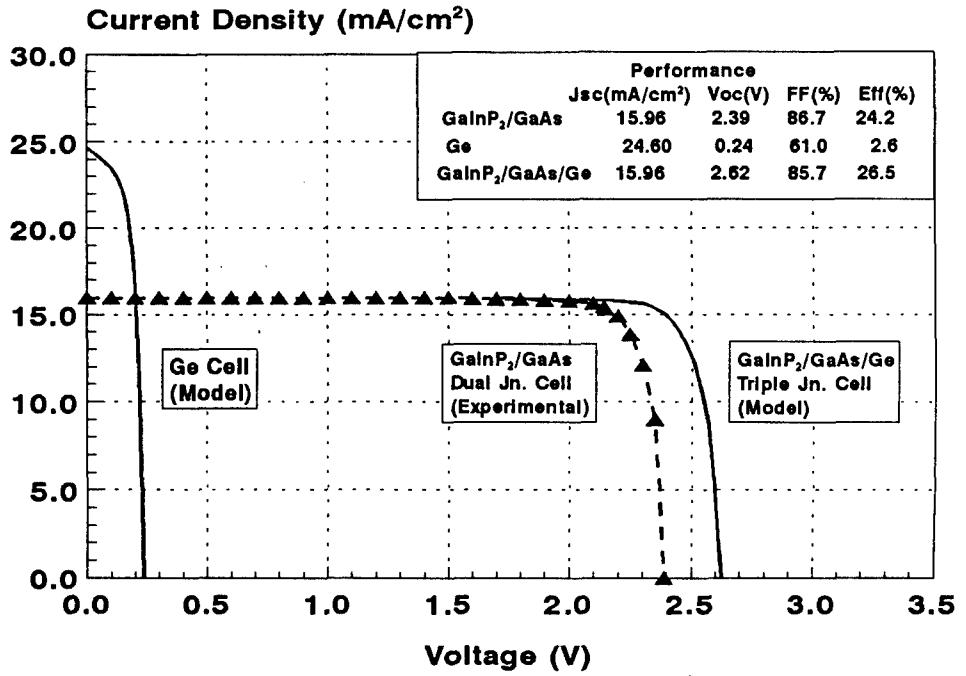

Figure 22. Modeled BOL performance of proposed n/p $GaInP_2$/GaAs/Ge monolithic triple junction cell (AM0 28 °C).

Spectrolab radiation models were also used to predict the "on orbit" operating performance of the triple junction cell in a typical geosynchronous environment. Previous work on the electron irradiation of Ge cells has demonstrated a low rate of current and voltage loss up to high fluence levels [1,2]. At an EOL fluence of 1×10^{15}, 1 MeV electrons/cm^2, the Ge cell continues to function as a voltage booster and the triple junction cell should achieve an EOL efficiency greater than 21.2%. Even with a higher rate of degradation with temperature, the triple junction provides significantly more power "on orbit" than the dual junction cell.

Table 2 summarizes the estimated operating temperatures in a geosynchronous orbit, at vernal equinox, for the $GaInP_2$/GaAs/Ge triple junction cell compared to a dual junction cell with and without a Controlled Reflectance Filter (CRF). These filters are used to reject infrared radiation in the wavelength range 900 nm to 1300 nm, that is used by the $GaInP_2$/GaAs/Ge triple junction cell but unused by the $GaInP_2$/GaAs/(Ge) dual junction cell.

Table 2. Multijunction cell operating temperature in geosynchronous orbit

Cell Type	Eff (%)(28°C)	Absorptance(%)	Temp(°C)
$GaInP_2$/GaAs/Ge (dual-junction)	24.0	89	54
$GaInP_2$/GaAs/Ge (dual-junction with CRF)*	23.8	77	40
$GaInP_2$/GaAs/Ge (triple-junction)	26.5	90	53

* CRF = controlled reflectance filter, e.g. IRR (PST) or BRR (OCLI)

These temperatures, in conjunction with estimated temperature coefficients for efficiency of -0.017% abs/°C and -0.032% abs/°C that have been determined for dual and triple junction cells, respectively, were used to generate Figure 23, that shows cell efficiency vs. operating temperature. Note that the temperature coefficients that were assumed for "optimized cells" at the time of the modeling, were subsequently found to be consistent with experimental data, obtained later in the contract.

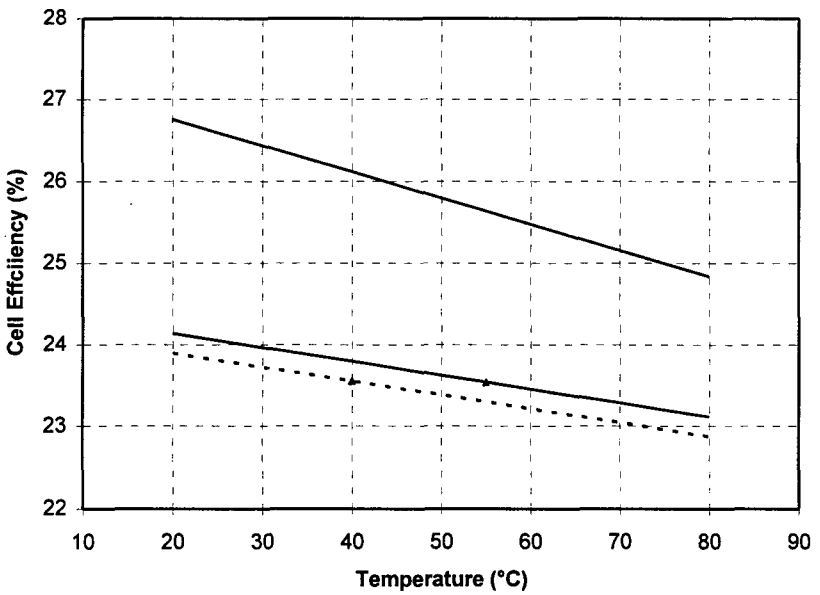

Figure 23. Modeled multijunction cell on-orbit operating performance.

At operating temperature, it was calculated that the triple junction cell provides an absolute efficiency improvement of about 1.9% over both the dual junction cell and the dual junction cell with CRF operating at a lower temperature. It should be noted that although the CRF affords lower absorptance of the CIC assembly resulting in lower operating temperature, this benefit is offset by the typical 1% current loss associated with the optical absorption in this type of filter.

3.3.2 Triple Junction $GaInP_2$/GaAs/Ge Cell Experimental Results

Following optimization of the MOVPE processes for fabrication of the discrete Ge cell and dual junction $GaInP_2$/GaAs cells, the task commenced to integrate all three junctions to achieve the fully monolithic triple junction $GaInP_2$/GaAs/Ge cell, previously shown in Figure 1. The target thickness of the emitter and base layers in the $GaInP_2$ cell were 0.1-0.15 μm and 0.4-0.48 μm, respectively. The carrier concentration in the emitter of both cells was $1\text{-}3x10^{18}$ cm^{-3}. The base of the top cell was doped to a level of $1\text{-}3x10^{17}$ cm^{-3}, while a base doping of the 3-6 x 10^{16} cm^{-3} was targeted in the GaAs cell to maximize EOL current collection. A high bandgap $AlInP_2$ layer was used to passivate the front of the $GaInP_2$ cell; the back surface was passivated with an AlGaInP layer. A $GaInP_2$ layer was used for the window on the GaAs cell and an AlGaAs (or $GaInP_2$) layer was used for back surface passivation. The Ge bottom cell active junction was formed by As diffusion into a p-type Ge substrate as previously described.

MOVPE growth of the $GaInP_2$/GaAs/Ge triple junction structure was performed using 3-inch diameter Ge substrates, since they represented state of the art in wafer size at the time this work was performed. The wafers showed mirror like surface morphology after layer growth. Wafers were then processed into 2 cm x 2 cm cells using standard single junction GaAs/Ge processing procedures. After processing, I-V curves were measured using an X-25 simulator intensity calibrated using JPL balloon flight $GaInP_2$ and GaAs (filtered by $GaInP_2$) standards. Since the short circuit current was determined by the top two cells (usually the $GaInP_2$ cell), and there was excess current generation designed into the Ge cell, a Ge standard was not used in the set up

procedure, since the measurement error introduced by excessive current generation in the bottom cell was calculated to be second order.

Figure 24 shows the IV curve data for the highest efficiency 2 cm x 2 cm cell fabricated under this task. The AM0, 28 °C efficiency, Voc, Isc, and Cff were 23.3%, 2.573 V, 58.06 mA and 86.1%, respectively. At the time of fabrication, this was believed to be the highest efficiency achieved for an n/p $GaInP_2$/GaAs/Ge triple junction cell.

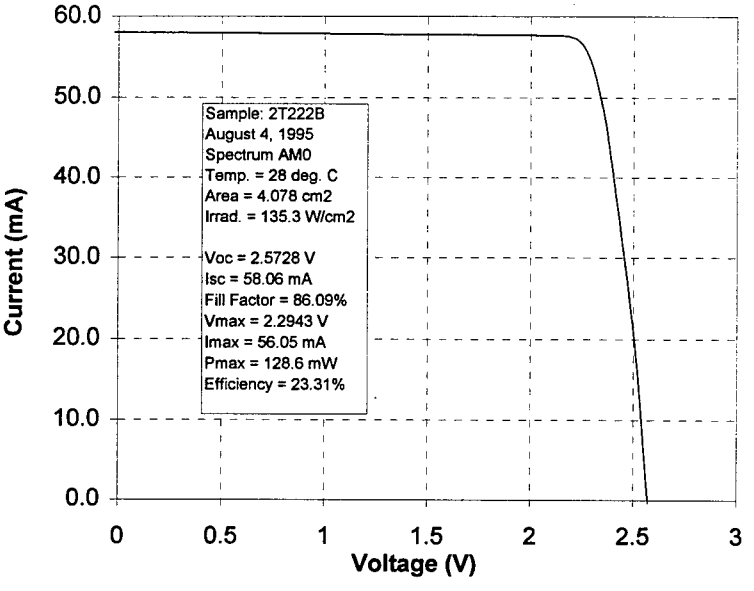

Figure 24. I-V curve for the highest efficiency $GaInP_2$/GaAs/Ge triple junction cell.

Figure 25 shows the measured cell efficiency distribution for 2 cm x 2 cm cells fabricated on a 3 inch diameter substrate. The average efficiency, Voc, Isc and Cff, measured across the wafer were 22.8%, 2.549 V, 58.1 mA and 84.7%, respectively, indicating that a large area cell, up to 4 cm x 6 cm, could have been fabricated. The spectral response was also measured at different wavelengths using a light bias technique. The external Q.E., and internal Q.E. (derived from the measured reflectance and external Q.E.), of the three subcells are shown in Figure 26. Integration of the external Q.E. with the AM0 spectrum confirmed excess current generation in the Ge cell and that that the triple-junction cell performance was limited by the top two cells.

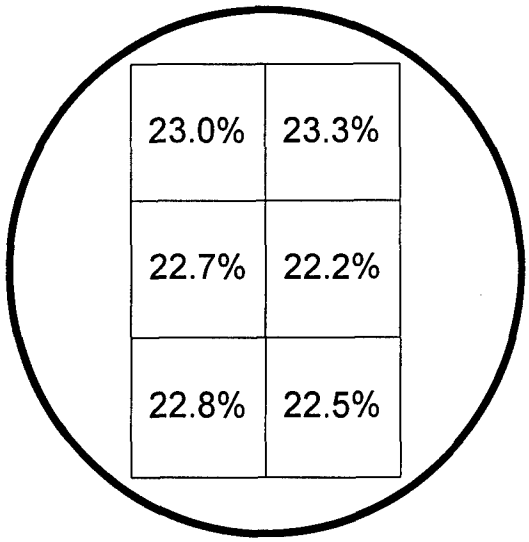

Figure 25. Efficiency distribution of triple-junction cells across a 3" diameter substrate.

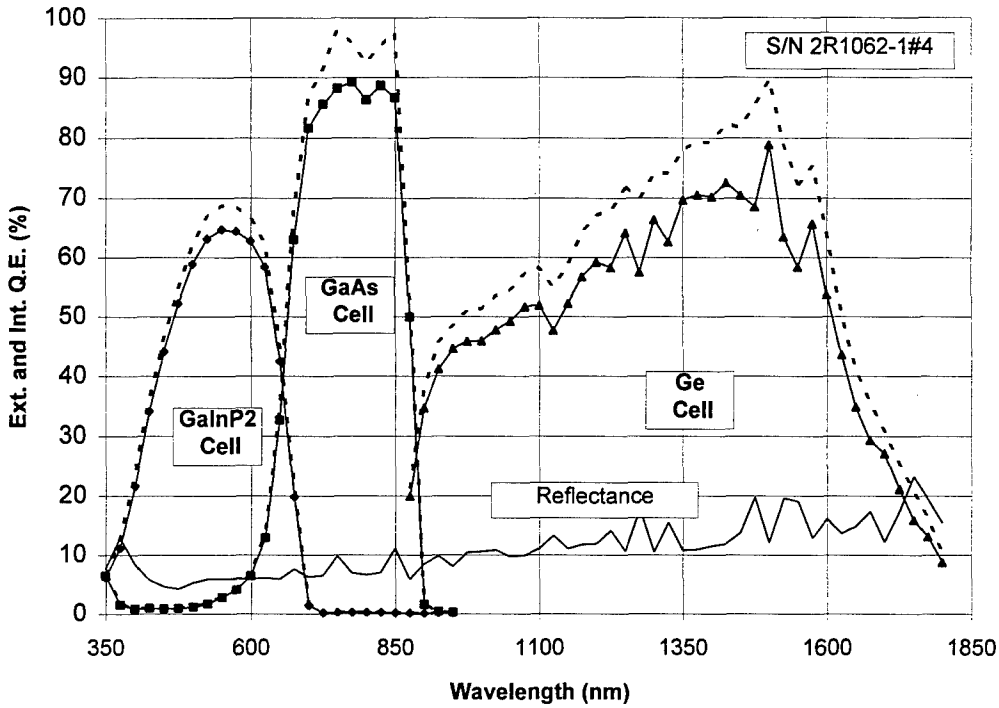

Figure 26. External quantum efficiency and reflectance of a triple-junction cell.

3.3.3 Triple Junction CIC Fabrication and Performance

A total of fifty-two (52) bare cells with an average efficiency of 22.1% were selected for the fabrication of CIC assemblies for delivery to Phillips Laboratory. Solid silver straps of 1 mil thickness, were attached to the top metal contact using a parallel gap welding process. Three mil thick, CMX glasses were then attached to the cell surface using Dow Corning DC 93-500 adhesive. Illuminated I-V testing was performed after completion of the CIC assembly to verify that performance was not affected by the welding or cell cover attachment processes. The highest CIC efficiency measured was 23.2% (AM0, 28 °C). The Voc, Isc, Cff were 2.564 V, 57.76 mA and 86.3%, respectively. The average efficiency for the 52 CICs was 21.94 %, which was very comparable to the average bare cell efficiency of 22.1% before they were fabricated into the CICs. The electrical performance for the 52 CICs that were delivered to Phillips Laboratory, is summarized in Section 3.4.

3.3.4 Triple Junction Cell Characterization Results

Triple junction cells were characterized by 1 MeV electron irradiation, measurement of temperature coefficients and stability after exposure to 30 day humidity testing. A triple junction cell was also flown on the JPL balloon flight of 1995, and its I-V curve was measured to verify the accuracy of ground testing. The same cell was also measured by NREL and Spectrolab. The efficiency measured from the balloon flight data was 0.7% and 1.9% (relative efficiency) lower than that measured by NREL and Spectrolab, respectively. This provided confidence for future triple junction cell testing. Thermal cycling test on triple junction CICs was also performed. No degradation in CIC performance was observed after one hundred (100) thermal cycles (-120 °C to +140 °C) were performed.

3.3.4.1 Electron Irradiation

A small quantity of bare cells were irradiated with 1.0 MeV electrons at a fluence up to 1E15 e/cm^2. After the irradiation, cells were re-measured using the X-25 simulator. The simulator

intensity was calibrated using the JPL balloon flight $GaInP_2$ and GaAs (filtered by $GaInP_2$) BOL standard cells.

The light IV results for the irradiated cells are summarized in Table 3. Voc1, Isc1, Cff1 and Eff1 are the open circuit voltage, short circuit current, fill factor and efficiency, respectively, for BOL. Voc2, Isc2, Cff2 and Eff2 are the results for EOL.

Table 3. Light I-V test results for BOL and EOL.

Device	Voc1 (V)	Voc2 (V)	Ratio	Isc1 (mA)	Isc2 (mA)	Ratio	Cff1 (%)	Cff2 (%)	Ratio	Eff1 (%)	Eff2 (%)	Ratio
2T101A-5	2.524	2.324	0.921	60.68	49.10	0.809	81.16	81.08	0.999	22.5	16.8	0.744
2T110A-5	2.526	2.342	0.927	60.66	49.35	0.814	83.67	82.42	0.985	23.2	17.3	0.743
Avg.	2.525	2.333	0.924	60.67	49.23	0.811	82.42	81.75	0.992	22.9	17.0	0.744

Average Voc, Isc, Cff and Eff ratios for cells measured at EOL to BOL were 92.4%, 81.1%, 99.2% and 74.4%, respectively. Since the ratio of Isc was very close to that measured in GaAs single junction cells, it was concluded that the EOL performance of the triple-junction cell was limited principally by the degradation of the GaAs cell. In order to verify this, spectral response measurements were performed on the cells. As shown in Figure 27 the external Q.E. for both $GaInP_2$ and GaAs cells degraded at EOL.

The ratio of integrated current for EOL to BOL were approximately 93% and 80%, respectively, for the $GaInP_2$ and GaAs cells, which confirmed that the EOL performance of current triple-junction cell was limited by the degradation of the GaAs cell. Further EOL performance improvements in triple junction cells are expected by improving the GaAs cell radiation resistance.

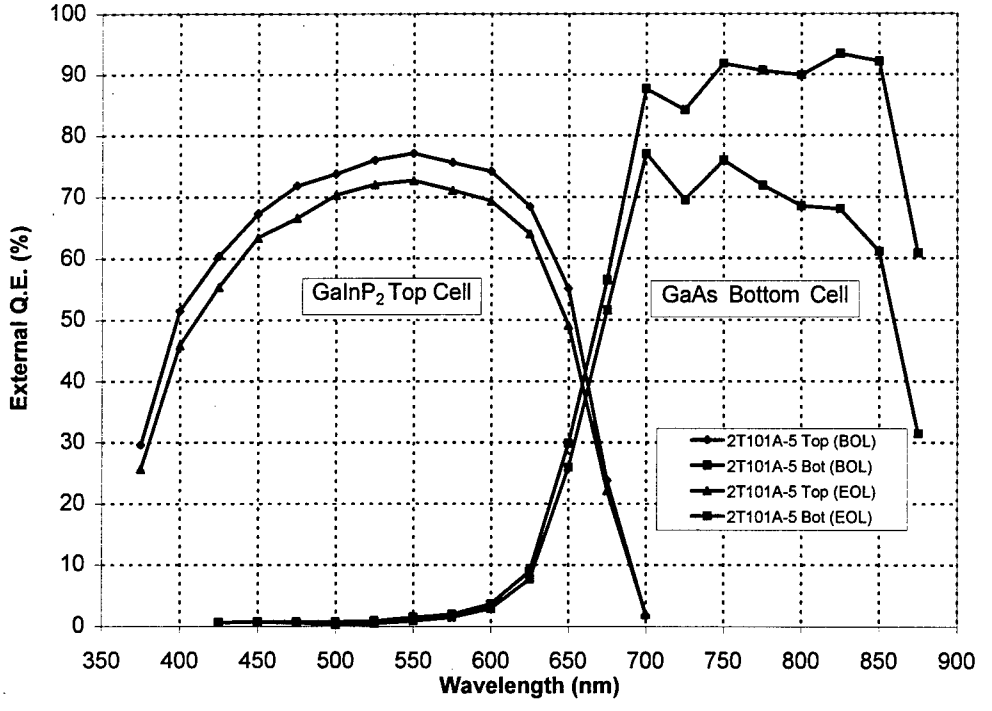

Figure 27. External quantum efficiency of a $GaInP_2$/GaAs/Ge triple junction cell measured before and after electron irradiation.

3.3.4.2 Temperature Coefficients

Temperature coefficient measurements were performed over the temperature range 10°C to 80 °C at four discrete temperatures of 10, 28, 50 and 80 °C. The results are summarized in Figures 28, 29 and 30. The variation of V_{oc} with temperature is shown in Figure 28. Open circuit voltage decreased with increasing temperature due to the rapid increase in diffusion and recombination currents with temperature. The rate of decrease of Voc with temperature was -6.07 mV/°C. For comparison, the temperature coefficient of 3.99 mV/°C for the dual-junction cell is also plotted in the same figure.

Figure 29 shows the variation of I_{sc} with temperature. The increase in Isc with increasing temperature is due mostly to the shift in the absorption edge of three cells. The rate of increase of short circuit current density with temperature was +0.0162 $mA/cm^2/°C$.

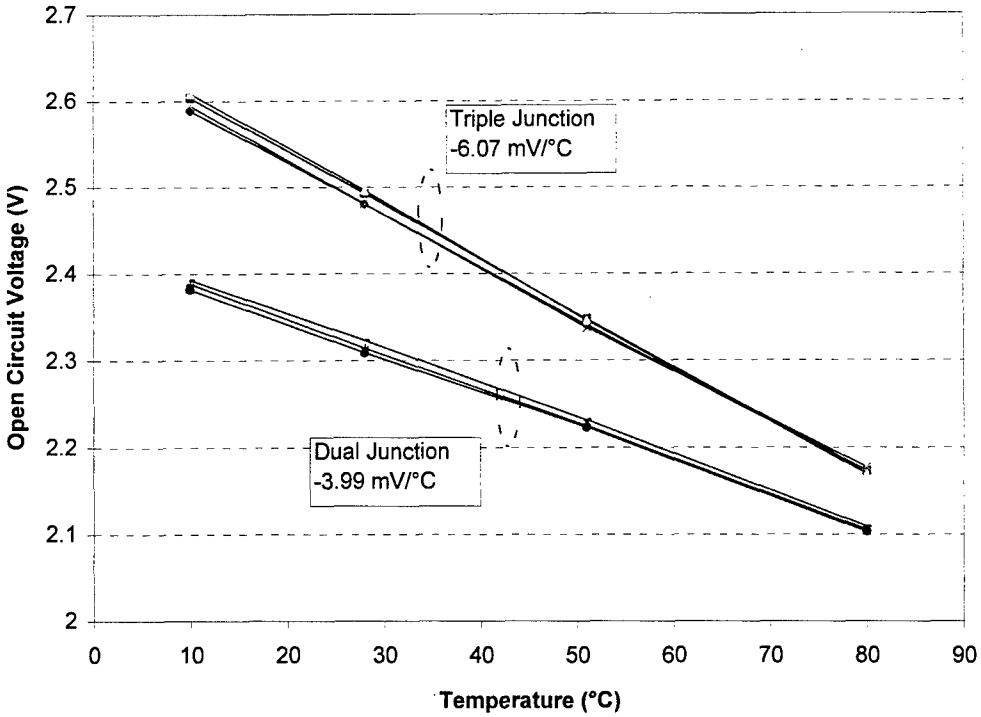

Figure 28. Open circuit voltage of dual and triple-junction cells as a function of temperature

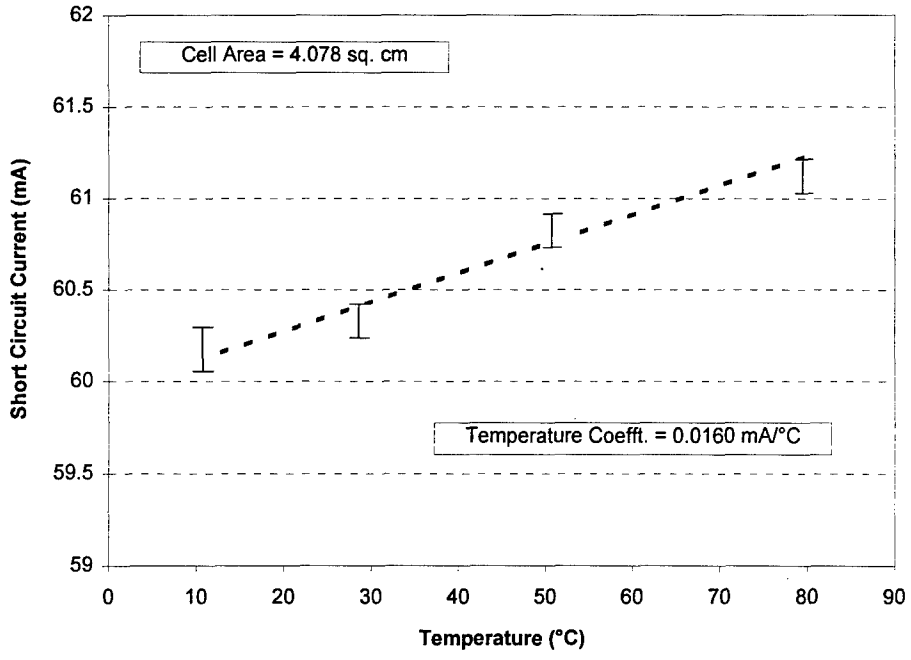

Figure 29. Short circuit current of triple junction cell as a function of temperature. (note: vertical bar in each temperature represents the range of measurements in three cells)

Figure 30 shows the variation of efficiency with temperature. Efficiency was found to decrease with increasing temperature for both dual and triple-junction cells. The measured rates of decrease of efficiency with temperature were 0.040 and 0.053 %/°C (absolute), respectively, for dual and triple junction cells. This figure also clearly shows the difference between these two devices is 2% absolute efficiency at an operating temperature of 54 °C [3].

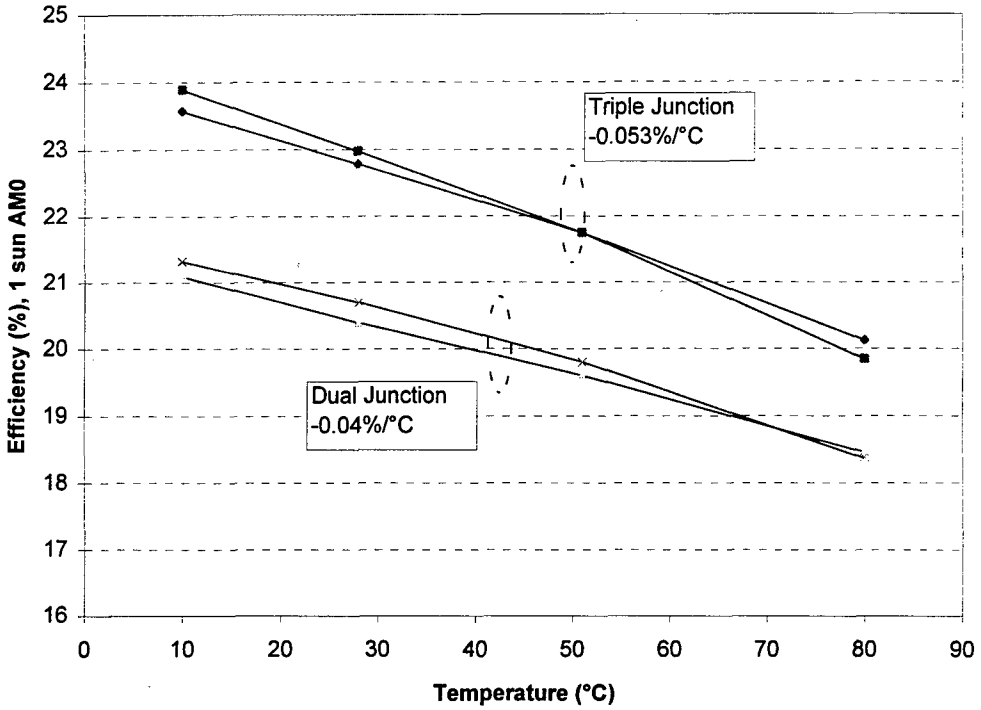

Figure 30. Efficiency of dual and triple-junction cells as a function of temperature

3.3.4.3 Humidity Test

AR coated dual and triple junction $GaInP_2$/GaAs/Ge cells were exposed to elevated temperature-humidity testing at a temperature of 45 °C and relative humidity >90% for a period of 30 days. Minimal degradation was observed in all of the tests, confirming the very stable nature of the top cell window material. The test data for AR coated dual junction GaIr GaAs/Ge cells are presented in Table 4. The bare cell degradation was on average 0.5% with a maximum cell degradation of 1.4%.

Table 4. Light I-V results for dual junction cells before and after 30 day humidity test.

Cell ID		Jsc (mA/cm^2)	Voc (V)	Cff (%)	Eff (%)	Eff(post)/ Eff(pre)
L082B4	Pre	15.5	2.312	80.7	21.4	
	Post	15.7	2.302	79.0	21.1	0.99
L082C1	Pre	14.6	2.326	86.1	21.6	
	Post	14.8	2.319	84.6	21.5	1.00
L082C2	Pre	14.6	2.344	85.3	21.5	
	Post	14.7	2.337	84.9	21.6	1.00

The data for AR coated triple junction cells are summarized in Table 5. Due to an unforeseen problem, the triple junction cell humidity test was terminated after 19 days. The 19 day humidity test result indicates the average efficiency loss for the triple junction cells was less than 1.5%.

Table 5. Light I-V results for triple junction cells before and after humidity test.*

Cell ID		Isc (mA)	Voc (V)	Cff (%)	Eff (%)	Eff(post) /Eff(pre)
3X328E2-4	Pre	60.0	2.447	79.1	21.2	
	Post	61.4	2.468	75.9	21.0	0.99
3X328E5-5	Pre	60.4	2.474	77.0	21.0	
	Post	60.4	2.434	76.2	20.5	0.98

* humidity test was terminated after 19 days

3.3.4.4 Triple Junction Balloon Flight Standard

Triple junction device measurements were performed using Spectrolab's modified X-25 simulator calibrated using balloon flight standards. The simulator had been previously modified with an attachment containing a set of movable filters that allowed trimming of the simulator's spectral content to achieve proper color balance between the $GaInP_2$ top cell to GaAs middle cell with respect to the set of balloon flight standards.

Cross correlation testing was performed between Spectrolab and NREL to verify the accuracy of Spectrolab mutijunction cell test methods. Device 2T110A4 was measured using this modified simulator with the appropriate set of top and middle cell standards. This cell was also measured at NREL using a multi-source filtering attachment. In addition to these measurements, cell 2T110A4 was mounted onto the standard JPL balloon package and flown on the 1995 balloon flight. The flight data, together with the temperature corrected data are shown in Table 6.

Table 6. Triple Junction Cell Testing Results

	Spectrolab Measurement (ASTM AM0)	JPL Balloon		NREL (WRRL AM0)
	Measured at 28°C	Measured at 53.5°C	Corrected to 28°C	Measured at 25°C
Isc	58.47 mA	59.98 mA	58.83 mA	58.97 mA
Voc	2.541 V	2.355 V	2.510 V	2.553 V
Eff	22.95%	21.15%	22.51%	22.6%
Cff	83.94%	81.96%	---------	83.89%

Measurement differences between Spectrolab ground and balloon measurements were less than 2%. Most of the error occurred in the voltage measurement, rather than Isc and fill factor. This error may be related to the difference in temperature coefficients of the measured cell and the values measured for other devices. Similarly, the difference between NREL and Spectrolab measurements was less than 2%. Good agreements in measured currents between the three measurements show that terrestrial measurements of multijunctions to within about 1% are possible.

3.3.4.5 CIC Temperature Cycling

Several CICs were subjected to 100 thermal cycles. In this test, the temperature varied from

-120 °C to +140 °C at the rate of 15 °C/min in each cycle. After the test, they were re-measured. The I-V results are very close to what were measured before the thermal cycle test indicating no degradation occurred during this thermal cycle test.

Four CICs were subjected to 100 thermal cycles with a temperature excursion from -120 °C to +140 °C at the rate of 15 °C/min in each cycle. The pre- and post- thermal cycle test data shown in Table 7, indicates that no degradation occurred during the thermal cycle test.

Table 7. Summary of the $GaInP_2$/GaAs/Ge triple junction CIC thermal cycling test results

	Voc1 (V)	Voc2 (V)	Ratio	Isc1 (mA)	Isc2 (mA)	Ratio	Cff1 (%)	Cff2 (%)	Ratio	Eff1 (%)	Eff2 (%)	Ratio
2T230A-1	2.481	2.478	1.00	55.27	55.93	1.01	81.45	81.02	0.99	20.25	20.36	1.01
2T230A-2	2.452	2.446	1.00	57.03	57.39	1.01	79.74	80.71	1.01	20.21	20.54	1.02
2T230A-4	2.482	2.476	1.00	56.61	57.21	1.01	78.52	78.27	1.00	20.00	20.10	1.01
2T231A-6	2.462	2.455	1.00	55.57	56.04	1.01	80.98	80.48	0.99	20.09	20.07	1.00
AVG	2.469	2.464	1.00	56.12	56.64	1.01	80.17	80.12	1.00	20.14	20.27	1.01

3.4 $GaInP_2$/GaAs/Ge TRIPLE JUNCTION CELL AND CIC DELIVERABLES

A total of seventy five (75) triple junction $GaInP_2$/GaAs/Ge cells were delivered to Phillips Laboratory in the latter phase of the contract. The electrical performance of the 75 cells is summarized in Table 8. The Voc, Isc, Cff and Eff distributions of these 75 cells are shown in Figure 31 through 34. The average Voc, Isc, Cff and Eff was 2.46 V, 60.4 mA, 80.8 % and 22.0 %, respectively.

Table 8. Summary of electrical performance of the 75 $GaInP_2$/GaAs/Ge triple junction cells. delivered (cells were grown in Spectrolab's large volume MOVPE system)

FileName	Voc(V)	Isc(A)	Cff(%)	Eff(%)
328E7-2	2.493	0.0606	84.06	23.18
328E4-4	2.490	0.0604	84.44	23.18
328E7-4	2.482	0.0607	83.63	23.00
328E3-3	2.492	0.0605	82.91	22.82
328E7-5	2.491	0.0608	82.53	22.82
328E4-1	2.486	0.0597	84.22	22.82
328E6-5	2.485	0.0618	81.39	22.82
328E4-2	2.484	0.0600	83.87	22.82
328E8-2	2.481	0.0606	83.14	22.82
328E3-2	2.484	0.0609	81.97	22.63
328E8-3	2.480	0.0604	82.78	22.63
328E6-6	2.476	0.0615	81.43	22.63
328E7-1	2.475	0.0605	82.81	22.63
328E4-6	2.498	0.0602	81.79	22.45
328E7-3	2.487	0.0604	81.88	22.45
328E4-3	2.485	0.0604	81.95	22.45
369E7-6	2.479	0.0607	81.08	22.38
369E2-6	2.462	0.0606	81.77	22.38
369E3-6	2.459	0.0610	81.33	22.38
328E7-6	2.491	0.0608	80.55	22.27
328E3-4	2.472	0.0610	80.91	22.27
369E8-5	2.473	0.0598	81.82	22.20
369E7-3	2.471	0.0598	81.89	22.20
369E2-5	2.462	0.0610	80.57	22.20
369E7-5	2.462	0.0604	81.37	22.20
369E10-6	2.461	0.0603	81.54	22.20
369E3-5	2.456	0.0614	80.24	22.20
328E4-5	2.502	0.0604	80.07	22.09
328E8-5	2.470	0.0605	80.97	22.09
328E3-1	2.466	0.0606	80.97	22.09
328E8-1	2.459	0.0601	81.88	22.09
328E6-3	2.457	0.0616	79.95	22.09
328E6-4	2.450	0.0641	77.05	22.09
369E2-2	2.450	0.0607	80.69	22.01
369E3-4	2.433	0.0607	81.26	22.01
328E3-5	2.481	0.0613	78.9	21.90
328E2-3	2.468	0.0596	81.58	21.90
369E8-2	2.471	0.0592	81.35	21.83
369E8-4	2.465	0.0599	80.59	21.83
369E9-5	2.463	0.0597	80.93	21.83
369E8-6	2.460	0.0600	80.62	21.83
369E10-5	2.453	0.0604	80.32	21.83
369E7-1	2.453	0.0595	81.53	21.83
369E3-3	2.449	0.0604	80.45	21.83

369E2-3	2.447	0.0604	80.51	21.83
369E10-4	2.438	0.0606	80.55	21.83
369E2-4	2.434	0.0612	79.89	21.83
328E5-2	2.457	0.0615	78.75	21.72
369E8-3	2.462	0.0590	81.23	21.65
369E8-1	2.461	0.0588	81.54	21.65
369E4-1	2.457	0.0591	81.26	21.65
369E9-4	2.456	0.0595	80.75	21.65
369E7-2	2.449	0.0598	80.57	21.65
369E10-3	2.448	0.0593	81.29	21.65
369E10-2	2.445	0.0603	80.04	21.65
369E9-6	2.445	0.0599	80.57	21.65
369E3-2	2.437	0.0603	80.30	21.65
369E6-3	2.432	0.0601	80.73	21.65
328E5-1	2.431	0.0611	79.44	21.54
369E7-4	2.455	0.0609	78.26	21.46
369E6-1	2.431	0.0601	80.08	21.46
369E6-4	2.430	0.0605	79.63	21.46
369E2-1	2.428	0.0605	79.65	21.46
369E9-1	2.440	0.0586	81.13	21.28
369E9-3	2.439	0.0593	80.20	21.28
369E9-2	2.438	0.0591	80.51	21.28
369E10-1	2.427	0.0605	79.00	21.28
369E3-1	2.415	0.0605	79.39	21.28
328E6-2	2.468	0.0641	73.33	21.17
369E11-3	2.447	0.0587	80.06	21.10
369E11-2	2.436	0.0586	80.56	21.10
369E11-4	2.419	0.0600	79.23	21.10
328E6-1	2.441	0.0640	73.61	20.99
369E6-2	2.421	0.0601	78.35	20.91
369E11-1	2.412	0.0586	80.65	20.91
Average	2.459	0.0604	80.77	21.96

*: Eff measurement error is $\pm$ 1%

The electrical performance of the 52 $GaInP_2$/GaAs/Ge triple junction CICs delivered to Phillips Laboratory are summarized in Table 9. The Voc, Isc, Cff and Eff distributions of these 52 CICs are shown in Figure 35 through 38. The average Voc, Isc, Cff and Eff in these 52 CICs were measured at 2.505 V, 59.17 mA, 81.34% and 21.94%, respectively.

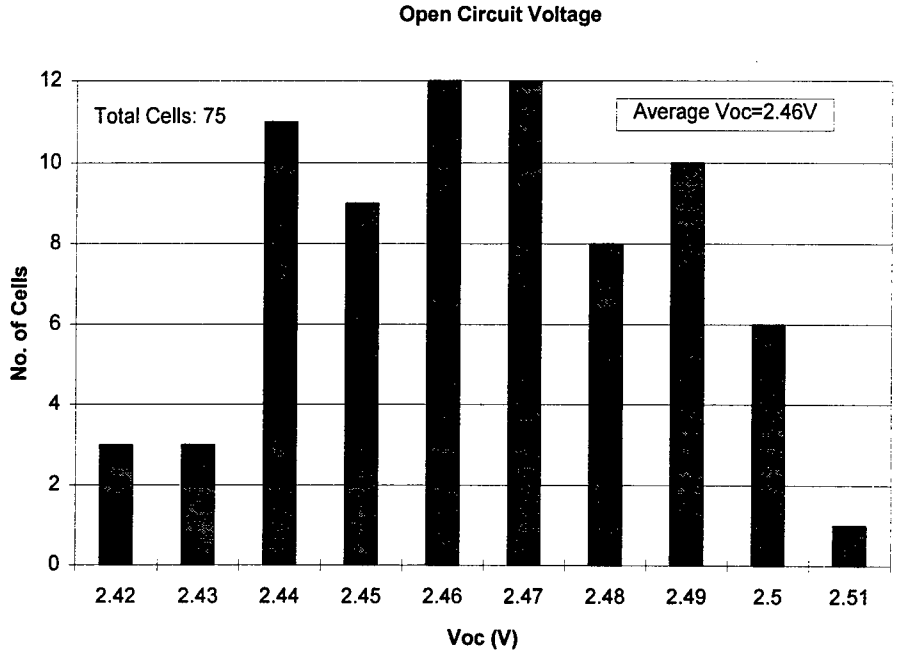

Figure 31. Voc distribution of the 75 cells shown in Table 8.

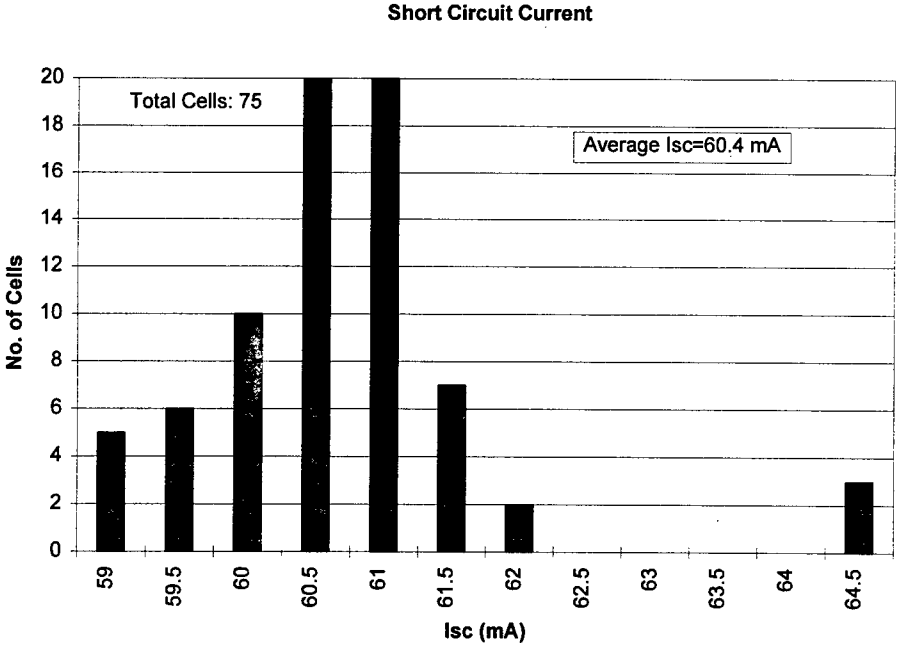

``Figure 32. Isc distribution of the 75 cells shown in Table 8.

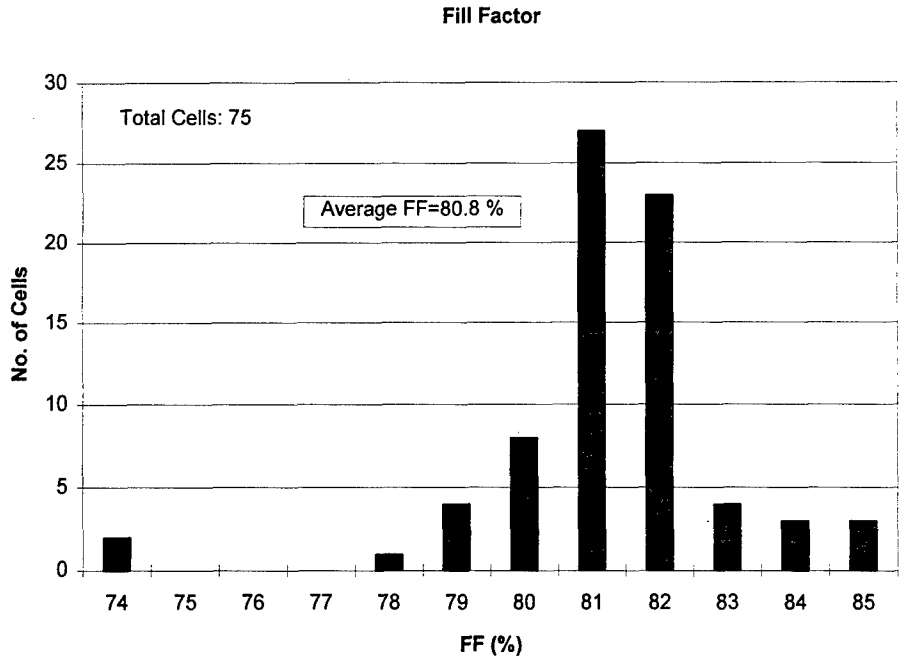

Figure 33. Fill factor distribution of the 75 cells shown in Table 8.

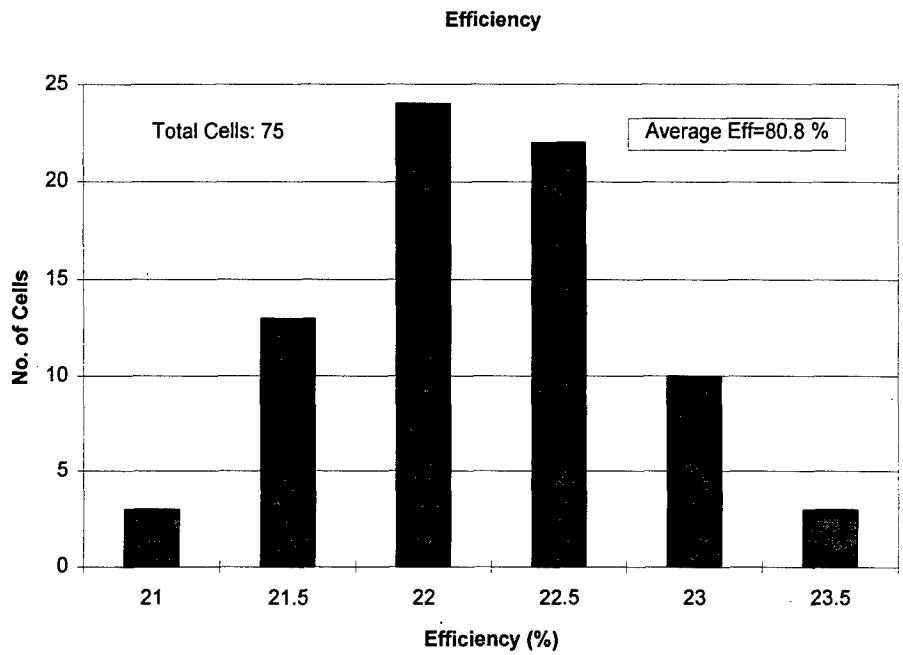

Figure 34. Efficiency distribution of the 75 cells shown in Table 8.

Table 9. Summary of electrical performance of the 52 $GaInP_2$/GaAs/Ge triple junction CICs delivered to Phillips Laboratory.

FileName	Voc(V)	Isc(mA)	Cff(%)	Eff(%)
2T084A-2	2.498	61.9	77.64	22.1
2T084A-5	2.530	61.6	75.84	21.7
2T084A-6	2.527	61.6	73.64	21.1
2T086A-2	2.538	62.3	79.77	23.2
2T086A-4	2.520	61.6	77.77	22.2
2T101A-2	2.497	61.7	79.36	22.5
2T101A-3	2.503	62.4	72.92	21.0
2T101A-4	2.506	61.8	77.63	22.1
2T101B-2	2.499	61.2	74.91	21.1
2T101B-5	2.546	62.1	77.36	22.5
2T110A-1	2.513	62.6	75.23	21.8
2T110A-6	2.518	61.5	74.81	21.3
2T110B-2	2.514	61.3	77.66	22.0
2T110B-5	2.488	60.4	79.93	22.1
2T110B-6	2.498	63.5	73.15	21.4
2T110C-1	2.499	62.3	76.43	21.9
2T115B-2	2.509	58.6	77.81	21.1
2T220A-1	2.512	57.1	81.08	21.1
2T220A-3	2.528	56.8	84.16	21.9
2T220A-6	2.533	60.0	81.30	22.4
2T220B-2	2.517	58.2	85.22	22.6
2T220B-4	2.511	60.1	80.00	21.9
2T220B-6	2.507	57.5	82.53	21.6
2T220C-2	2.480	58.3	81.35	21.3
2T220C-3	2.489	58.2	81.76	21.5
2T222B-1	2.555	58.0	85.22	22.9
2T222B-2	2.516	58.0	84.51	22.4
2T222B-3	2.519	58.6	82.96	22.2
2T222B-4	2.564	57.8	86.31	23.2
2T222B-5	2.527	58.4	82.61	22.1
2T222B-6	2.514	57.6	84.09	22.1
2T222C-2	2.463	59.3	79.46	21.0
2T222C-3	2.480	57.2	84.62	21.8
2T222C-4	2.437	57.3	83.24	21.1
2T222C-5	2.462	56.9	84.66	21.5
2T222C-6	2.482	58.3	84.42	22.2
2T230A-5	2.436	56.8	82.49	20.7
2T231A-2	2.480	56.4	87.02	22.1
2T231B-2	2.483	56.4	86.24	21.9
2T231B-3	2.479	55.7	85.83	21.5
2T231B-5	2.472	56.2	82.82	20.9
2T231B-6	2.479	56.6	85.22	21.7
2T309A-2	2.511	59.1	83.92	22.6
2T309A-3	2.513	59.0	84.81	22.8

2T309A-6	2.507	57.7	84.43	22.2
2T309B-1	2.513	58.7	81.42	21.8
2T309B-2	2.518	59.4	84.20	22.8
2T309B-3	2.520	58.7	85.18	22.8
2T309B-4	2.515	58.1	85.83	22.7
2T309B-5	2.509	57.9	83.81	22.1
2T325A-4	2.536	59.3	83.03	22.6
2T325A-6	2.508	58.9	82.09	22.0
Average	2.505	59.2	81.34	21.9

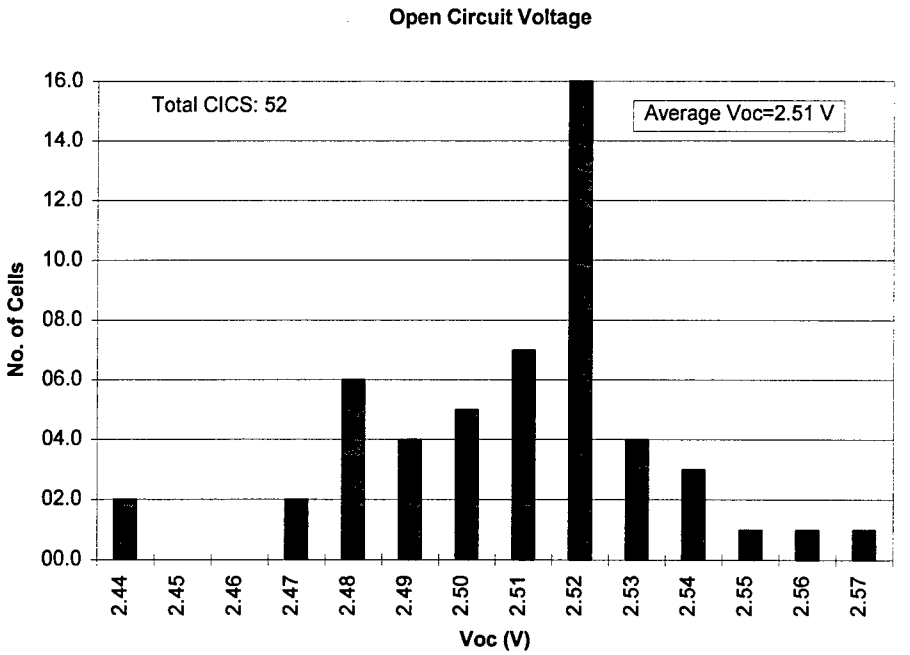

Figure 35. Voc distribution of the 52 CICs shown in Table 9.

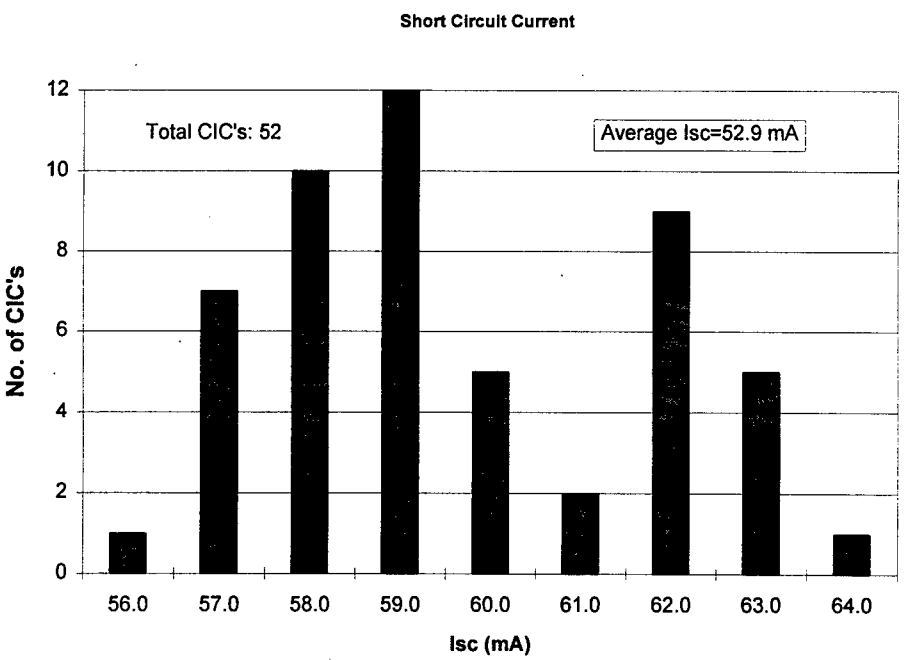

Figure 36. Isc distribution of the 52 CICs shown in Table 9.

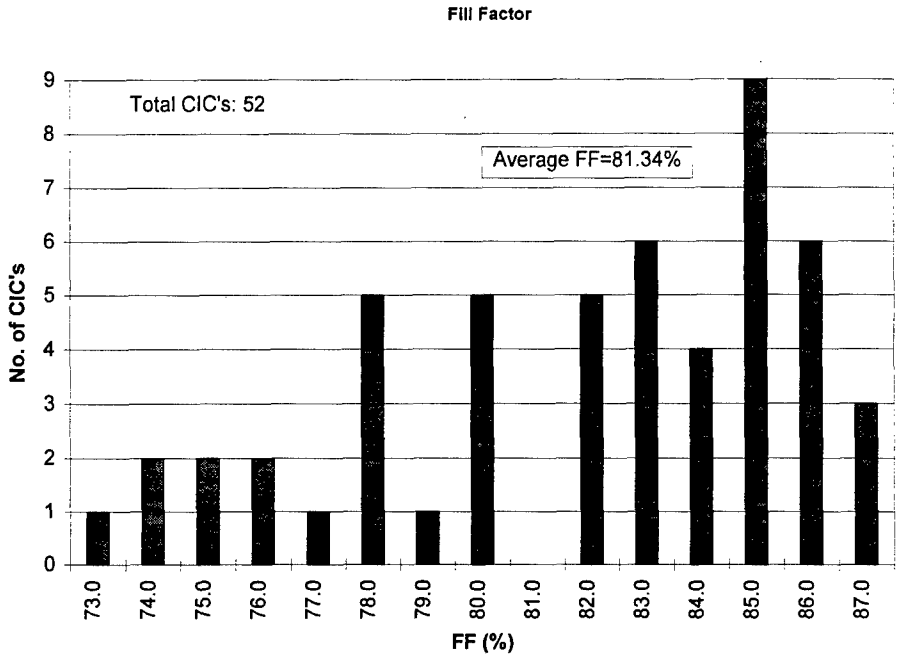

Figure 37. Fill factor distribution of the 52 CICs shown in Table 9.

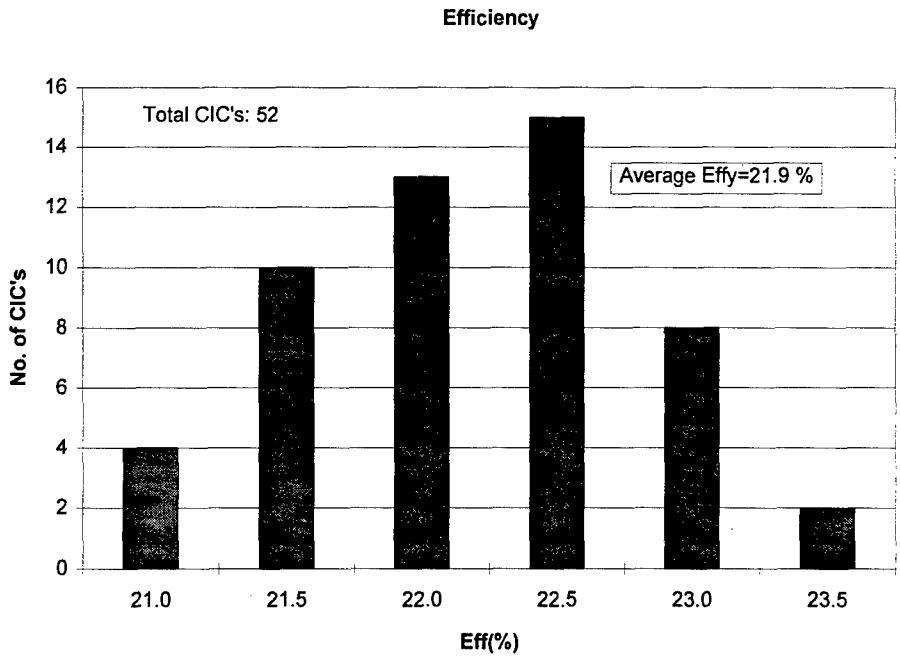

Figure 38. Efficiency distribution of the 52 CICs shown in Table 9.

4.0 CONCLUSIONS AND RECOMMENDATIONS FOR FUTURE RESEARCH

This highly successful program has demonstrated the feasibility of cost effectively manufacturing dual and triple junction $GaInP_2$/GaAs/Ge cells and integrating them onto a space flight power system. The highest efficiency 2 cm x 2 cm triple junction cell fabricated was 23.3% (AM0, 28 °C). This was the highest reported efficiency for a monolithic triple junction cell at that time. Electron irradiation of a small population of cells showed that remaining EOL power of approximately 75% BOL (P/P_0 =0.75) may be achieved on the triple junction cell after radiation with 1 MeV electrons to a fluence of 1E15 cm^{-2}. Further improvements to the GaAs middle cell are possible that are expected to improve to P/P_0 to 0.80 at 1.0 MeV (1E15 e/cm^2) electron irradiation. Temperature coefficient measurements show approximately a 2% absolute efficiency difference between the dual and triple junction cells at an operating temperature of 54 °C indicating that the triple junction cell will find application in many flight systems.

Triple junction CIC assemblies were also successfully fabricated and delivered to Phillips Laboratory, in[illegible]ting the "transparency" of the product to Spectrolab's standard welded panel fabrication processes. The best CIC (2 cm x 2 cm) efficiency was 23.2%. No degradation in CICs was observed after 100 thermal cycles were performed.

A total of seventy five (75) bare cells and 52 CICs were delivered to Phillips Laboratory to fulfill the contractual obligations for this program.

Finally, an analysis of the factors limiting the average efficiency of the cells was performed. Several low risk improvements for optimization of the cell design and/or fabrication process for future research have been identified. A tabular summary of these parameters, with estimates of performance improvements to be achieved, is shown in Tables 10 and 11. The antireflection coating changes are assigned a very high probability for success. Improvements to the $GaInP_2$, GaAs, and Ge cells, including a higher band gap top cell, a more effective BSF in the GaAs cell, and improved surface passivation and bulk quality in the Ge cell, are regarded as low risk

improvements to the current devices. With these improvements, the triple junction cells will be capable of providing a minimum average efficiency of 26.5% in volume production.

Table 10. Incremental efficiency improvements identified for $GaInP_2$ and GaAs cells.

	Efficiency % Average AM0, 28 °C	Efficiency % Maximum AM0, 28 °C
PRESENT CELLS	21	22.5
IMPROVEMENTS		
Higher Index DAR	21.3	+0.3
Blue Response	21.6	+0.3
Thickness Tuning	21.9	+0.3
Doping Optimization	22.4	+0.5
Higher Band Gap Top Cell	22.7	+0.3
Reduced Defects / cm^2	24.3	+1.4
Efficiency of DJ Cell after the Improvements	24.3	25.6

Table 11. Incremental efficiency improvements identified for Ge cells.

	Efficiency % Average AM0, 28 °C	Efficiency % Maximum AM0, 28 °C
PRESENT CELLS	Insufficient database	1.8
IMPROVEMENTS		
Surface Passivation		+0.2
Wafer Quality Improvements		+0.3
Reduced Shunt Resistance		+0.3
Efficiency	2.2 (est.)	2.6
Efficiency of TJ Cell after Improvements Identified in Table 3-10 above)	26.5	28.2

5.0 REFERENCES

[1] R. Venkatasubramanian et. al., "High temperature performance and radiation resistance of high efficiency Ge and $Si_{0.07}Ge_{0.93}$ solar cells on lightweight Ge substrates", Proc. 22nd IEEE PVSC, 1991, pp.85-89.

[2] D. D. Krut et.al., "The development of Ge bottom cell for monolithic and stacked multijunction applications", Proc. 22nd IEEE PVSC, 1991, pp. 90-92.

[3] P.K. Chiang et.al., "Large area $GaInP_2$/GaAs/Ge multijunction solar cells for space applications", Proc. 1st world conf. on PV energy conversion, 1994, pp. 2120-2123.

DISTRIBUTION LIST

AUL/LSE Bldg 1405 - 600 Chennault Circle Maxwell AFB, AL 36112-6424	1 cy
DTIC/OCP 8725 John J. Kingman Rd, Suite 0944 Ft Belvoir, VA 22060-6218	2 cys
AFSAA/SAI 1580 Air Force Pentagon Washington, DC 20330-1580	1 cy
PL/SUL Kirtland AFB, NM 87117-5776	2 cys
PL/HO Kirtland AFB, NM 87117-5776	1 cy
Official Record Copy PL/VTV/1Lt David Keener Kirtland AFB, NM 87117-5776	2 cys
PL/VT Dr Hogge Kirtland AFB, NM 87117-5776	1 cy